**Guilherme Miguel Melo Coelho**

Bachelor of Science in Micro and Nanotechnologies Engineering

# Wearable Integrated Devices for Sustainable Energy: Self Powered e-Cloths

Dissertation submitted in partial fulfillment of the requirements for the degree of

**Masters in Micro and Nanotechnologies Engineering**

| | |
|---|---|
| Advisor: | Dr. Sumita Goswami, Senior Researcher, AlmaScience |
| Co-Advisor: | Prof. Luís Miguel Nunes Pereira, Associate Professor, DCM, FCT-UNL |

Examination Committee:

| | |
|---|---|
| Chairperson: | Prof. Rodrigo Ferrão de Paiva Martins, Full Professor, DCM, FCT-UNL |
| Raporteur: | Prof. Manuel João de Moura Dias Mendes, Assistant Professor, DCM, FCT-UNL |
| Member: | Dr. Sumita Goswami, Senior Researcher, AlmaScience |

December 2020

FACULDADE DE CIÊNCIAS E TECNOLOGIA
UNIVERSIDADE NOVA DE LISBOA

**Wearable Integrated Devices for Sustainable Energy: Self Powered e-Cloths**

# Acknowledgements

Em primeiro lugar, gostaria de expressar os meus agradecimentos á instituição que me permitiu concluir esta fase da minha vida, a Faculdade de Ciências e Tecnologias da Universidade NOVA de Lisboa. Não posso deixar de agradecer aos elementos que compõem o CENIMAT e CEMOP que ajudaram ou apoiaram, de uma maneira ou outra, a construção e execução desta tese. Agradeço também á Professora Doutora Elvira Fortunado e Professor Doutor Rodrigo Martins, que são as mentes por detrás deste curso. Obviamente, tenho que agradecer especialmente ás pessoas que estiveram mais perto de mim durante a realização deste trabalho, Sumita Goswami e Suman Nandy pela orientação no trabalho e por todos os seus conhecimentos nas mais diversas áreas, Guilherme Ferreira pelas muitas horas passadas no laboratório a acompanhar-me e pela participação ativa no planeamento e construção do módulo de comunicação "wireless", que faz parte deste trabalho, e queria agradecer ainda ao André Opinião. Por fim, não posso deixar de agradecer em particular ao Professor Luís Pereira por me permitir trabalhar neste projecto.

Em relação aos agradecimentos mais pessoais, tenho que começar pelas pessoas que sempre estiveram comigo nesta longa caminhada: a minha família. Obrigado pais por serem a maior inspiração da minha vida e por me terem disponibilizado tudo o que sempre necessitei para dar por completa a minha vida académica, até este ponto. Obrigado Carolina pelo apoio e exemplo de excelência que sempre me demonstraste, por me teres sempre ensinado a ser uma pessoa melhor e por todas as nossas confidências e brincadeiras que só os irmãos compreendem. Por fim, obrigado aos meus familiares de quatro patas que me acompanharam durante estes cinco anos da minha vida, Pepita, Picas e Odin. Vocês trazem-me sempre um sorriso!

Queria agora agradecer á minha namorada, uma das melhores coisas que a faculdade me deu. A todo o teu apoio incondicional, ajuda e amor só posso estar imensamente agradecido.

Agora, aos amigos que a faculdade me trouxe! Em primeiro lugar, obrigado ao meu melhor amigo Dmytro pelos anos de partilha da experiência que foi a nossa faculdade, com muitas horas em jogos, estudos e parvoíce. Obrigado Recife por juntos termos "construído a nossa casa" e por todos os grandes momentos que passámos. Agradeço também a todos os outros inquilinos da Casa 1, Olga e Marta. Casa 1 para sempre. Agradeço ao Zé, Diogo Patrício e, novamente, Dmytro por todos os épicos momentos dos "Mo Boys" que irei guardar para sempre na minha memória. Um especial obrigado também aos elementos do mítico "Segundo Esquerdo" Rui, Madeira e Carvalho. Gostaria também de agradecer á Raquel, Eduardo, Tomás, Ricardo, Nuno, João Pedro, Filipe Lopes e Pedro Mourarias pessoas pelas quais ganhei muito carinho. Por fim, mas não menos importante, quero agradecer á Nia, Margarida, Kika, Juju, Xavi, Inês, Bruno, Luis, Moniz e todos aqueles que em algum momento me ajudaram na minha caminhada.

Fora da faculdade tenho que agradecer especialmente ao meu melhor amigo de infância que sempre me acompanhou durante todos estes anos, Micael Gomes. Obrigado Filipe, Martim, Pedro, Patrícia, Andreia, Renato Vale, Miguel, Vasco, Cristiana, Joana, Chavez e Falhuscas por todos os momentos que partilhámos enquanto fomos crescendo juntos.

# Resumo

Atualmente, as novas tecnologias "wearable" estão a mudar a maneira como comunicamos uns com os outros e com as máquinas. Neste trabalho é explorada a ideia da utilização de fibras têxteis comerciais, funcionalizadas com Polipirrole como material ativo, para a construção de dispositivos electrónicos capazes de gerar energia a partir de movimentos mecânicos. Polipirrole faz parte da família dos polímeros conjugados. A principal ideia por detrás do funcionamento dos dispositivos criados neste trabalho é o mecanismo de tranferência de cargas e tranferência de energia, que se foca na interface entre o polímero conjugado em contacto com metal (elétrodo), quando existe uma força externa aplicada no sistema. Com isto, foi possível a criação de tecidos utilizando as fibras têxteis funcionalizadas com polipirrole, que geram currente quando sofrem ação de movimentos mecânicos humanos. Os melhores resultados conseguidos neste trabalho em relação á densidade de potência e densidade de corrente foram 2.29 $W/m^2$ e 23.9 $mA/m^2$, respectivamente. Com o melhor dispositivo produzido fomos capazes de acender instantaneamente 50 LEDs ligados em série. Com este dispositivo também fomos capazes de carregar 1 V num condensador de 33 µF em 225 segundos. Os dispositivos criados demonstraram estabilidade eléctrica durante os 6 meses de testes a que foram submetidos e como principal aplicação foram utilizados na deteção de movimentos humanos.

Palavras-Chaves: Conversor de energia mecânica; Polipirrole; Dispositivos Electrónicos "Wearable"; Mecanismo de Tranferência de Cargas; Polímeros Conjugados.

# Abstract

Nowadays, from lifestyle to sports and health to security, wearable technology is an inevitable trend that, through the human-machine interaction, has the capability of transforming businesses by making them smarter, more informative, and more communicative. In this study, commercial textile fibers have been functionalized with Polypyrrole (PPy) to achieve an electronic system that can convert external mechanical energy into electrical energy. PPy is a biocompatible π-conjugated polymer. The main principle behind the devices' operation is the charge transfer mechanism that occurs between the π-conjugated polymer and the metal (electrode) layer when the system suffers mechanical stress. Furthermore, the PPy functionalized textile has been weaved to an e-cloth, through a custom-built weaving machine. This e-cloth can generate current under human-motion interaction. The best results achieved in this study, in terms of power density and current density, were 2.29 $Wm^{-2}$ and 23.9 mA $m^{-2}$, respectively. Considering the best device, we were able to light up to 50 LEDs connected in series. With this device, we were also able to charge a 33μF capacitor up to 1V, in 225 seconds. All the devices built have kept electrical stability during the six months of the work. The main application explored in this study was the detection of human movements through motion interactive energy harvesting technology.

Keywords: Mechanical Energy Harvester; Polypyrrole; Wearable Electronics; Charge-Transfer Mechanism; Conjugated Polymers.

# Table of Contents

# List of Tables

# List of Figures

# List of Abbreviations

AC - Alternating Current

APS - Ammonium Persulfate

D-MM – Device Metal Metal

D-MMC – Device Metal Metal Cotton

DC – Direct Current

DI Water – Dionized Water

e-textile – Electronic Textile

EDS - Energy Dispersive Spectroscopy

FESEM - Field Emission Scanning Electron Microscopy

HCl - Hydrochloric Acid

HTTP - Hypertext Transfer Protocol

IoT – Internet of Things

$I_{sc}$ – Short Circuit Current

PC – Portable Computer

PDMS - Polydimethylsiloxane

PPy- Polypyrrole

SDCC - Stress-Deliverer and Charge-Collector

SEM - Scanning Electron Microscopy

SSID - Service Set Identifier

TENG – Triboelectric Nanogenerator

UART - Universal Asynchronous Receiver/Transmitter

$V_{oc}$ – Open Circuit Voltage

# List of Symbols

I – Current

P – Power

V – Voltage

R – Resistance

eV – Electronvolt

# Motivation and Objectives

Today we live in extraordinary times, with unprecedented advancement and development in science and technologies. In the last decades, the increase of the human population and our mass consumption lifestyle, backed by new powerful technologies, has led to some massive environmental problems and an economic crisis that the world had never witnessed before. Henceforth, it is of uttermost importance to find and invent new solutions and technologies that can enable us to have the same lifestyle as today, while having a powerful but positive impact in terms of environmental sustainability.

Most of the energy used today come from conventional fossil fuels! The energy consumed in industry, services, households, and transportation are the largest source of green house gases (75%) [1]. Therefore, it is an urgent requirement to take a step towards green and sustainable power source technologies, while supporting a circular economy. European Green Deal Investment Plan will mobilize at least €1 trillion in sustainable investments over the next decade, indicating a serious demand for green technology [2]. The majority of the renewable energy sources are based on solar, wind, hydroelectric, geothermal or biomass [3]. But, with the increasing usage of flexible and portable devices, there is a great demand for finding smart and green ways to create and store energy so that we can use our low power wearable electronics in the most variable ways. Therefore, the biggest technical challenge is to manufacture sustainable and portable power source that can feed electrical power uninterruptedly at the power levels of micro-to-milliwatts. This situation projects the next generation of self-powered technology, that will operate without any external power! Such self-powered devices are integrated with energy harvesting and transducing systems, where energy is harvested from ambient sources (mechanical, solar, humidity, thermal, wind, fluid flow, etc.), by directly transforming these energies into electrical energy [4]. Among them, mechano-responsive energy harvester is considered as one of the most available and ubiquitous energy sources, because it can harvest energy from daily wastage of mechanical energy in form of any kind of motion, vibration, and touch, independent of seasons and weather. It can be used spontaneously without using storage device, which can be very useful for wireless signal mechanism or tracking system. In the last few years, there has been a lot of research in this area and there are promising results that take advantages of human motions and heat to harvest energy [5].

This study is a contribution to the investigation of fresh and greener renewable energies. Here we explore the habilities of some materials that can harvest mechanical energy, powered by human motion and movements. This is a new step for us, as humans, to be able to produce energy by ourselves to power small gadgets that everybody uses every day, like cellphones, cameras, music players, and even power banks. In this type of technology, it is important that the devices are totally self-powered, that is, they produce their own energy to work and do not need other external energy supplies.

# 1 Introduction

## 1.1 e-Textile:

In the 21st century, technology is emerging more stylish, where the new generation is paying more attention towards trendy and fashionable wearable gadgets. At the same time, essential sectors like health and defense are demanding ultra-advanced, flexible, and smart textile technology for more prosperity [6]. Technologists are using a combination of sensors, machine learning and big data analysis to provide consumers data about their bodies and lives, more than ever before. On the other side, the human body is rich in mechanical energies that are being wasted in form of body movement. Power generation that comes from breathing, heating, blood transport, arm motion, and walking can reach over 100 W for an average 68 kg adult's daily activities [6]. Therefore, this wastage energy can be converted into electricity, through smart textiles, for powering various electronics. This can open a new door for electronic textiles (e-textile) which will accumulate energy dissipated by the daily body movements and convert it into sustainable electrical energy through high-performance e-cloth systems and embedded high-performance human-machine interface systems.

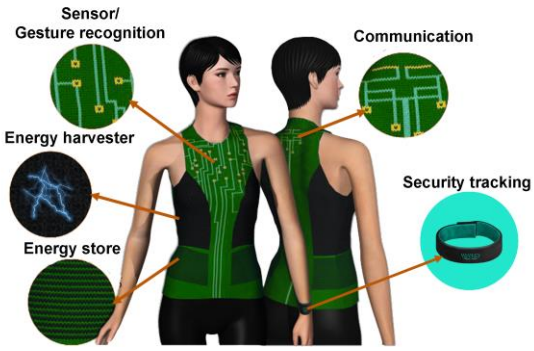


**Figure 1.1** *Schematic of possible applications of electronic textiles.*

The "e-Textile" or "e-Cloth" is defined when traditional textile products (such as fibers or yarns forming woven, knitted, or non-woven structures) are combined with electronics either through integration or functionalization that can interact with the environment or user [7]. Wearable electronics based on textiles refer to a wide area of research and technologies that enhance the versatility of fabrics. Due to the specific features of textiles such as flexibility, light weight, and wearability, as well as their intrinsic warm and fit properties, electronic textiles seem to be highly appropriate to be implemented in the next generation of smart electronic communications and energy harvesting applications. The implementation of electronics in common fabrics can be very important for the creation of smart materials. These types of materials have a broad variety of functions and applications such as microprocessors, batteries, sensors, communication units, displays and energy harvesting. In this way, smart materials can help us to have a better life quality and to have a better management of our time, economy, and resources, meanwhile helping in environmental sustainability [8]. Due to all these advantages and opportunities, it is expected that the smart textile market will increase exponentially its valor in a near future. The latest reports claim that the global market value of smart textiles in 2019 was 802.3 million US$ and it is expected to reach the value of 8139.2 million US$ by 2027, even with the COVID-19 lockdown impact [9].

One of the most important aspects and major challenge about e-textiles technology is how these smart devices communicate between themselves and with other external devices. Since the goal of the e-textiles is to implement electronics in our fabrics in a comfortable and practical way, there are some problems in using wired connections. Therefore, the best option to use in this type of devices is wireless communication [10], something that was implemented in the applications sector of this work (**sector 3.5.3**).

## 1.2 Mechanical Energy Harvester: A Concept of Green Energy

With advent of smart technologies and materials (e.g. e-Textile), portable devices and related power supplies have become a centre of research nowadays. Whereas it is also important to develop green energy systems for a better and sustainable future. Both these priorities are being quite fulfilled through energy harvesters. Among various types of such energy harvesters (solar, thermal, etc.), the mechanical energy harvesters are our point of interest during this thesis work.

There are mainly two mechano-responsive energy harvesting systems that are trending for smart eletronics investigation: piezoelectric and triboelectric effects. The nature of the piezoelectric effect is closely related to the generation of electric dipole moments in solids upon exerting external stress that generates electricity [11]. The dipole moments may either be induced by ions on crystal lattice sites or by their own asymmetric charge distribution structure. The most common materials that are being used for piezoelectricity are lead zirconate titanate (PZT), barium titanate and lead titanate. Gallium nitride and zinc oxide are also hugely used as piezoelectric semiconducting materials due to a relatively wide band gap, that can generate an instantaneous polarisation inside their lattice on the application of a force. On the other hand, the fundamental working principle of the triboelectric effect is a kind of contact electrification and electrostatic induction between two different materials when rubbed, forced, or slid to each other [12, 13]. Contact electrification can be described by the process of charge transfer between two materials that are brought together and separated, providing static polarized charges and electrostatic induction between two materials that convert mechanical energy into electricity [14]. Based on the materials, the contact-separation triboelectric is mainly divided into two categories: dielectric-to-dielectric and conductor-to-dielectric. However, the triboelectric phenomenon is not yet totally understood by the scientific community. The thecnology sometimes differs from materials to materials.

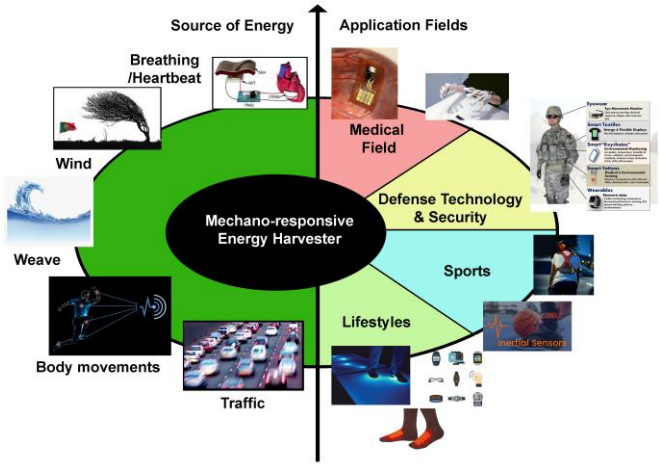


**Figure 1.2** *Mechano-responsive energy harvester: wasted mechanical energy that has been used into electrical energy and applied to various smart applications.*

In the past few years, scientists have devoted considerable work into the development of triboelectric nanogenerators (TENGs). It is a new research trend related to power supply and energy harvesting that can offer a lot of new possibilities and has already some applications. The most important thing is that this nanogenerator device architecture can easily be combined with textile fibers or cloth that can be further incorporated into everyday life. This combination has a lot of potential advantages because it blends the versatility, light weight, biocompatibility, and flexibility of the textiles with good electrical performance [15-16]. There are

two different types of textile-based TENGs: the fabric-based TENG (the structure is a common fabric that is modified at its composition level to be electrically active or to be the substrate of electrically active material) and the fiber-based TENG (the structure can be only one or more individual textile fibers that are modified to be electrically active) [17].

In terms of fiber-based mechanical energy harvesting devices, the past few years have brought a great variety of investigations. Apart from the fiber-based TENGs (referred to in the previous paragraph), other types of promising devices also incorporate textile fibers that is the fiber-based piezoelectric nanogenerators (FPENGs), the fiber-based thermoelectric generators (FTEGs), and even the fiber-based electret nanogenerator (FENG) that harvest mechanical energy through electrostatic induction. A lot of research is being done on fiber-based mechanical energy harvesting, with promising results among all the different kinds of devices, as can be seen in **Table 4** (Annex 1. section) where demonstrates some recent state-of-the-art devices and respective output results.

## 1.3 Charge Transfer Mechanism

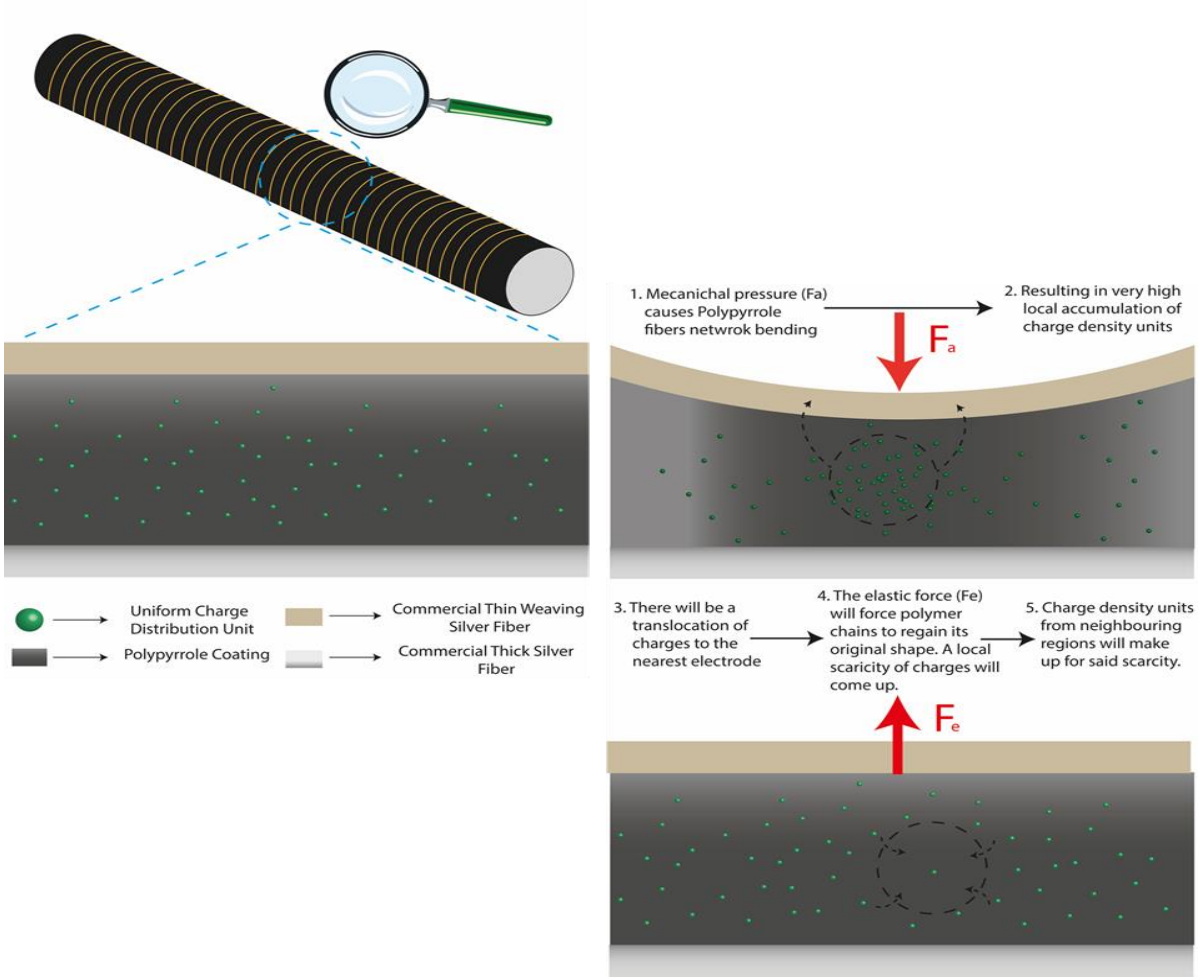


**Figure 1.3** *Schematic of the charge transfer mechanism proposed in this work.*

In this study, we used conjugated polymers (which are not conventional triboelectric materials) as the mechano-stimuli energy harvester. Generally, undoped PPy shows an insulator behavior with a large band gap of approximately 3.16 eV. Upon oxidation (doping of PPy), the formation of two narrow bipolaronic bands decreases the energy gap approximately from 3.16 eV to 1.4 eV (**Figure 6.1** in **Annex 2.**) [18].

The energy harvesting system of this work is focused on the charge transfer that occurs in the surface between the π-conjugated polymers and the metal (electrode), upon a mechanical response. When mechanical stress is applied to the system, there is a molecular structure deformation in the polymer chains which results in a local squeezing between molecular chains, causing an excessive density of electrons. This rise in electrons density causes a local Fermi level pinning. Hence, the pinned electrons will migrate to the nearest energy level available, which is the metal, creating a peak current. Moreover, and when the mechanical stress is released, the polymer networks expand and there is a local shortage in electrons (depinning of the local Fermi level). As PPy now behaves like a conductor, the localized electrons scarcity will be compensated by the electrons in the adjacent regions through hopping mechanism, creating a smaller current peak with the opposite polarization from the first, since this carriers transfer is done in the opposite direction. By the end of this process, it is possible to start a new mechanical stress cicle that originates a new peak current [14,19]. **Figure 1.3** represents a visual schematic of the charge transfer mechanism.

## 1.4 Conjugated Polymers

Conductive polymers are very interesting for both industrial and research applications due to their excellent electrical conductivity, thermal stability, easy synthesis, and ecological stability [20-21]. These types of polymers are conductive due to delocalized π-electrons arising from the overlapping of p-orbitals [22]. Because of this special and unique chemical characteristic, many scientists and researchers are interested in conductive polymers and their present and future applications [23]. Up to this date, conjugated polymers have been used for applications like PLEDs (Polymer Light-Emitting Diodes) [24], field emission [25-27] and electrochromic displays [28-29], sensors [30-31], biosensors [32-33] and biomedical applications [34-35], among others [36]. Also, some of them, like polypyrrole and polyaniline, are reported to be used for energy harvesting purposes namely in supercapacitors, pseudocapacitors, rechargeable batteries, and flexible storage devices [32,37]. In most of these reports, those polymers were applied in the different systems as electrodes, but in some recent research, they are also being used as an active layer material [14,19].

Before this study, our work group explored polyaniline as an active material to generate electrical power, achieving very promising results [14,19]. But there are other conjugated polymers that can generate energy, like Polypyrrole, PEDOT (poly(3,4-ethylenedioxythiophene)), and polyacetylene.

Polypyrrole (PPy) is the conductive polymer that is explored during this study, for energy harvesting applications. It offers electrical semiconductor/metal properties and at the same time has the physical properties of normal polymers like flexibility and elasticity [38]. The chemical and physical properties of PPy can be easily controlled through doping-dedoping processes. Furthermore, the pyrrole monomer has good environmental stability and great redox properties that make it easy to oxidize. It is also soluble in some common solvents including water, and easily available product in the market. Besides, PPy is also reported to have a high conductivity value as polyaniline. All these properties make PPy one of the most studied conductive polymers and a great contender for organic electronics materials [39].

# 2 Materials and Methods

## 2.1 Main Reagents

Pyrrole monomer (98%, Sigma-Aldrich), ammonium persulfate (APS; 99.99%, Sigma-Aldrich), and hydrochloric acid (HCl; ~37%, Alfa Aesar) are the main reagents used in the synthesis of polypyrrole (PPy). All the reagents were used as received without any further purification. Throughout all the experiments and washing procedures, only deionized (DI) water was used (obtained from Millipore Elix Advantage 3 purification system).

## 2.2 Polypyrrole (PPy) Synthesis

Two precursor solutions were prepared to synthesize PPy: the monomer solution and the oxidant solution. To make the monomer solution, we added 200 µl of pyrrole monomer to 20 ml of DI water and stir for 10 minutes. For the oxidant solution, we added 1.3 g of ammonium persulfate (APS) to 10 ml of DI water and let it stir until the solution became homogeneous in about 5-10 minutes. After the solution became homogeneous, we added 125 µl of hydrochloric acid (HCl) and let the solution stir again for 10 minutes. The two solutions were put in an ice bath for 20-30 minutes to reach 0ºC. After that, the monomer solution was added to the oxidant solution with gentle stirring, and the mixed solution was placed in the ice bath again for a determined time, which will be further explained below.

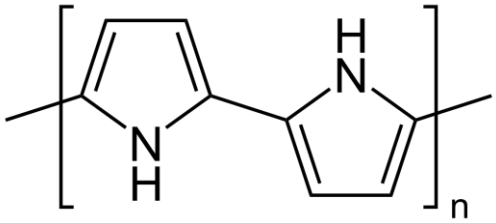


**Figure 2.1** *Polypyrrole neutral chemical structure.*

## 2.3 Functionalization of Textile Fibers

After the optimization of the PPy synthesis process, the goal was to functionalize textile fibers with PPy. For this purpose, silver-coated commercial textile fiber was used as a substrate, with a diameter of 400 µm. Small pieces of silver-coated commercial textile fibers (11 to 12 cm average length) were dipped into the final PPy mixture solution (as obtained following the process above) for functionalization through *in-situ* polymerization technique. Not all the fiber's length was inside the solution, leaving some spare space to create a metal core contact. Given that, an average length of 1.5 cm was left above the reactant solution, using Kapton tape to glue this part of the fiber to the beaker's inner wall. During the current study, we used three different functionalization times for the fibers: 30 minutes, 60 minutes, and 90 minutes. After the stipulated time, the fibers were removed from the reaction vessel. A uniform black coating throughout the surface of the fibers was clearly observed, demonstrating the successful chemical deposition of PPy. Later, the PPy coated fibers were washed with DI water (to remove the excess of PPy material and unreacted reagents as well) and were stored

in the lab for a few days to dry them properly before making the energy harvester system. Moreover, it is important to note that the remaining PPy aqueous solution was filtered and then the filtrate was kept in the normal oven at around 60ºC for 24 hours, to finally collect the PPy powders to perform chemical analysis with it.

To see if the above procedure could be easily upscaled, 1-meter average length fibers were also functionalized through *in-situ* polymerization technique. The chosen PPy functionalization time was 30 minutes.

## 2.4 Fabrication of the Fiber-based Energy Harvesting Devices

After the PPy-functionalized fibers were completely dried, we started assembling the energy harvesting devices. Each functionalized fiber was wrapped up with a different number of windings with another commercial silver-coated conductive textile fiber (125 µm diameter). This way, the uncoated metallic end of the thicker fiber (part of the fiber that was above the PPy solution) was used as one electrode to reach the polymeric part, and the other electrode was obtained from taking contact to the thinner metal-coated fiber on the other side. To cover and protect the functionalized fibers, we used PDMS (polydimethylsiloxane) elastomer to curing agent considering a ratio of 10:1. The curing was performed at 60°C. The fibers were attached with copper tape to make extended contacts out of the PDMS cover for connecting the device to the electrical measurement systems.

## 2.5 Characterization Techniques

Morphological and compositional analyses were conducted by using a field emission scanning electron microscope (FESEM-FIB, Carl Zeiss Auriga Crossbeam microscope) with energy dispersive x-ray spectroscopy (EDS, Oxford XMax 150). The chemical structures of the samples were also characterized by Raman spectroscopy (Renishaw Qontor InVia Raman microscope), using the 532 nm excitation laser line with 10% of the maximum laser power (50 mW) and 1s exposure time for every 10 accumulations. The mechanoelectrical studies were performed by recurring to a standard oscilloscope (TektronixTBS 2022).

# 3 Results and Discussion

## 3.1 Chemical and Morphological Analyses

In this study, one of our main objectives was to properly functionalize textile fibers substrates with polypyrrole (PPy). The properties of synthesized PPy can be manipulated through the amount of oxidization of the monomer to form the polymer chain and that can be achieved by different methods, like using different oxidants or changing the time of polymerization of the monomer (one of the variables studied in this work).

Synthesized conjugated polymers are normally insulators and the essential mobile charge carriers for electrical conduction are produced only via oxidation (*p*-doping) and, more rarely, through reduction (*n*-doping). This doping is achieved by chemical or electrochemical methods. In the reduced state, PPy acts as an insulator, but in the oxidized state, PPy is positively charged [40].

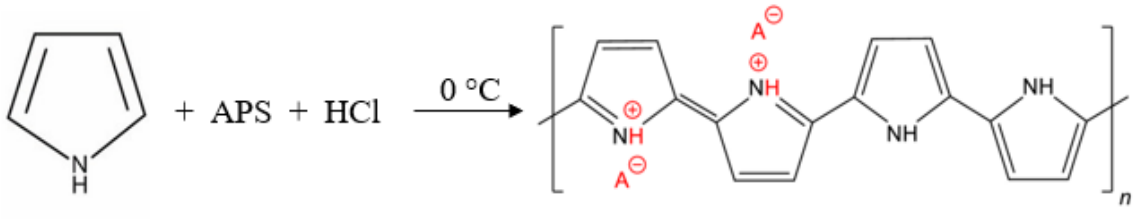


**Figure 3.1** *Schematic of the chemical reaction of polypyrrole reproduced in this work. The red "A–" in the schematic represents the dopant anion.*

With a 3.6 eV band gap, the undoped PPy is a dielectric. When oxidated, the *p*-electrons are extracted from the upper level of the valence region with a simultaneous change to lower energies of the boundary *p*-levels (the highest occupied and the lowest vacant). The band gap decreases to around 1.4 eV and the PPy gains the electrical properties of a semiconductor [40].

The method of charge transfer is of particular importance in PPy electrical conduction. Polarons and bipolarons produced upon doping are the charge carriers (**Figure 3.2**). In chemical terms, the formation of a polaron is equivalent to the formation of a radical cation, as well as the bipolaron formation is equivalent to the dication formation. The polaron and bipolaron in PPy are extended structures spread over three to four monomeric units of the chain.

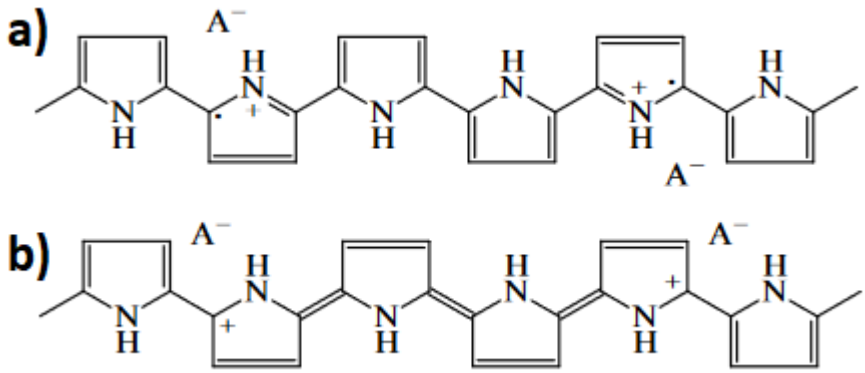


**Figure 3.2** *a) Formation of the polaron; b) Formation of the bipolaron [39]*

The energy of the system is affected by the separation of the positive charges in the bipolar configuration. The further away the positive charges are from each other, the greater is the decrease of system stability, as it produces more unstable quinoid rings. Recent investigations have found that the polarons and bipolarons have the same mobility in the PPy chain, so they contribute similarly to the conductivity of PPy [40].

In this study, we used APS as the oxidant agent, although there are other oxidant agents reported to work as well, such as ferric chloride and iron sulfate [41]. The purpose of choosing APS as oxidant was because of its high oxidation potential. The oxidant not only compensates the charge of the free charge carriers but also enhances the probability of interchain charge transfer due to a strong overlap of the atomic orbitals of the oxidant, with the p-orbitals of the carbon atoms.

Herein, we also added HCl that according to some reports greatly enhance the conductivity of PPy at low concentrations [42].

### 3.1.1Raman Spectroscopy

Raman spectroscopy was performed to check the chemical properties and the structure fingerprint of the synthesized polymer. The samples used in the Raman tests were the powder collected from the precipitate produced during the fiber functionalization process. Three different powders were tested, each one with a different time of polymerization (30 minutes, 60 minutes, and 90 minutes).

**Figure 3.3** shows the Raman spectra of the powders collected from the different polymerization times. It is clear from the spectra, that the chemical phases from all the polymerization times are similar in characteristics and correspond to the successful formation of PPy having all its typical characteristics peaks [43], as expected. The strongest peak is observed at 1576 $cm^{-1}$ wavenumber which corresponds to the symmetric stretching of aromatic C=C ring of PPy, that represents the oxidation state. Other peaks were around 928 $cm^{-1}$ and 967 $cm^{-1}$ which are associated with the ring deformation caused by the bipolarons and the polarons species, respectively. It was possible to observe two more peaks, one associated with the C—H in plane deformation of the oxidized PPy (1047 $cm^{-1}$) and the other associated with the ring stretching mode of the PPy chain (1331 $cm^{-1}$).

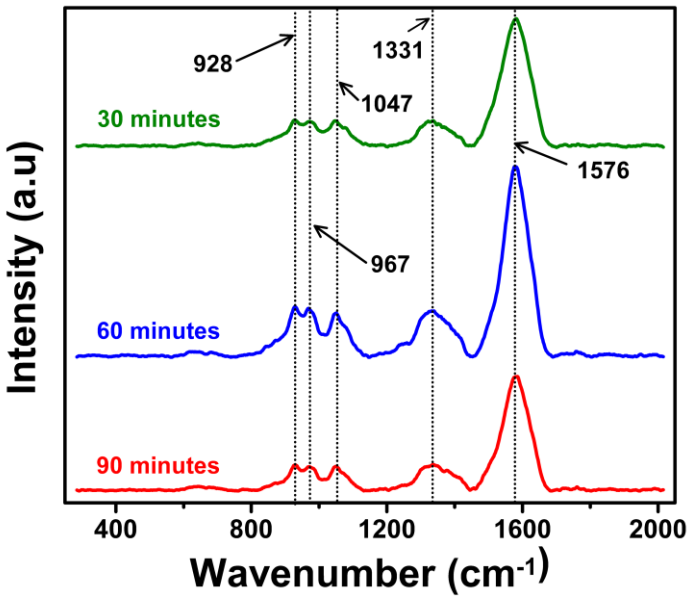


**Figure 3.3** *Raman Spectroscopy results of PPy powders with different polymerization time i.e 30,60 and 90 minutes. The symmetric spectra show that as a chemical structure all the PPy was in same phase.*

### 3.1.2 SEM Images

**Figure 3.4** shows the SEM images of the PPy-functionalized textile fibers for different polymerization times and the corresponding high-resolution images from the PPy nanostructure surfaces. From the high-resolution SEM image, it can be observed that the textile fibers were coated with PPy that has granular nanostructures, with 80-120 nm in average size. However, no significant morphological difference was noticed for PPy with different polymerization times. The only possible difference is in the thickness of the coating (that is not shown in the figure), which can eventually increase with polymerization time. It is worthy to mention that during present thesis work no study related to the thickness of this coating was performed, as our group (in its previously published work with polyaniline [14,19]) has noticed that the charge transfer process in such polymer/metal interface systems is a surface phenomenon and presumably happening in the localized surface area where the pressure or stress is implemented or released.

The corresponding EDS elemental mapping (using Oxford XMax 150) of the typical PPy functionalized fiber is illustrated in **Figure 3.5**. A strong presence of Ag (silver) was noted because of the commercial conducting textile fiber which has been used as the core substrate for functionalization. Chlorine was also present in great quantity because of the addition of HCl during the synthesis of PPy, which increases the presence of anionic $Cl^{-}$ dopant in the polymeric chain. Carbon is one of the components of PPy. Oxygen (although in lower quantity) came from the environment and sulphur was also present because the oxidant agent used in the synthesis of PPy was APS.

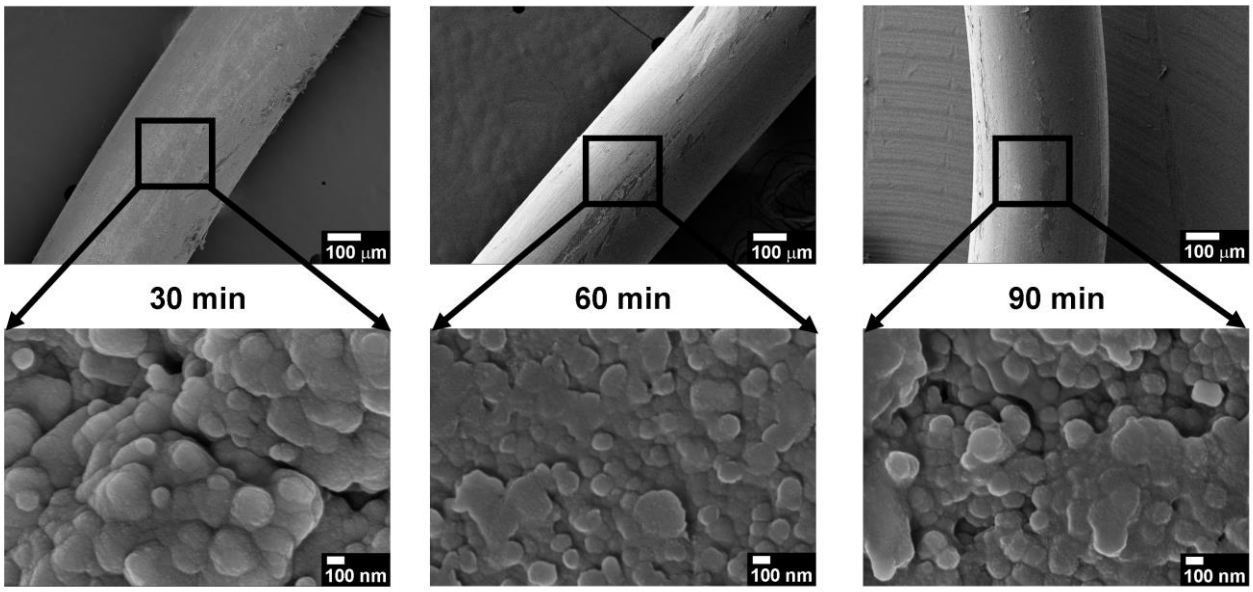


**Figure 3.4** *SEM images of the PPy functionalized textile fibers. The different times of functionalization are represented: 30 minutes, 60 minutes, and 90 minutes (from left to right). On the top, is represented the fibers coated with PPy, and at the bottom, the corresponding high-resolution SEM images.*

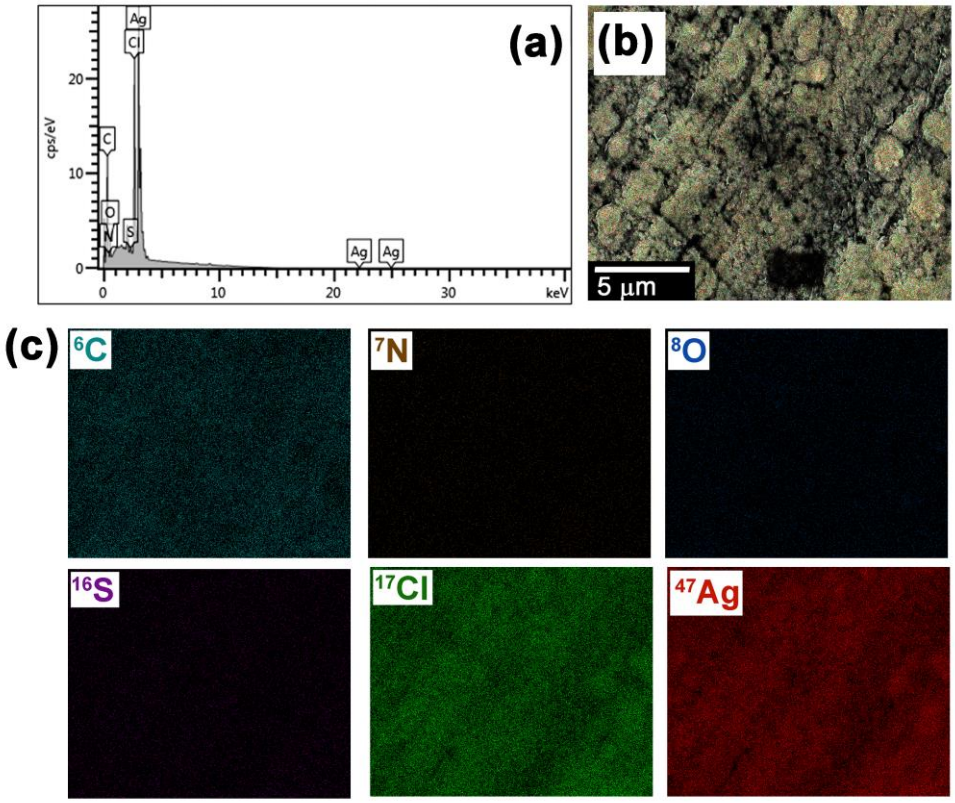


**Figure 3.5** *EDS test performed in the 60 minutes textile fiber functionalized with PPy. a) EDS spectrum, b) EDS layered image, c) EDS elemental mapping.*

## 3.2 Electrical Analysis of Textile-based Energy Harvester

For the textile-based energy harvester design, a series of steps were performed: the functionalized PPy fibers were wrapped up with another silver conductive fiber (with lower diameter) and then integrated in parallel. The thinner conducting fiber was implemented to act as a stress-deliverer and charge-collector (SDCC) electrode. Another electrode was created as back electrode (the metallic layer of 400 diameter textile fiber, where the PPy has been functionalized). The commercial copper tape was used to extend the connections related to thinner and thicker electrodes. All the harvesting devices have the same PDMS packing area (around 120 $cm^2$), the fibers used have 11 cm in length, and the copper electrodes length varies from 7 to 9 cm. **Figures 3.6 (a)** and **(b)** show the schematic design of the energy harvesting device and a schematic of a single wrapped fiber. **Figure 3.6 (c)** shows the image of a prototyped device.

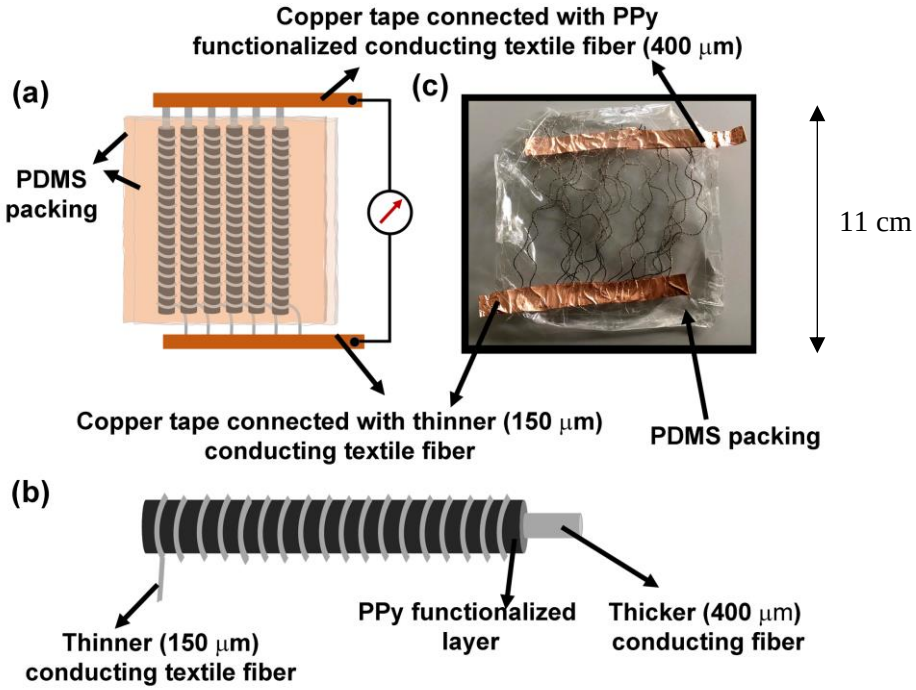


**Figure 3.6** *The schematic design of (a) the prototyped device (b) single wrapped fiber; and (c) the digital image of a prototyped device.*

To obtain the main electrical parameters of the fibers, we constructed a harvesting application platform. Also, we recorded the open-circuit output voltage ($V_{oc}$) and short-circuit output current ($I_{sc}$) of the devices. Thus, the device was put under stress and release sequences, pressing it with the hand at a constant force and frequency (hand patting). When stressing the conductive fibers, a forward output signal is generated. This happens due to the mechanical stress that the metal/PPy interface layer suffers. The charge transfer mechanism will be initiated in the interface by localized fermi level pinning caused by the charge density accumulation in the stressed area, where the PPy chains get shrunk together. Contrary, when releasing the mechanical stress, a reverse output signal is produced. This can be explained according to the localized Fermi level depinning stage. There is a local scarcity of charge carriers (that were transferred during the stress-induced period) and to obtain the electrostatic stability, the charge carriers will hop from the ruptured polymeric area (through the back electrode) or nearby polymeric areas through tunneling process. Therefore, the generated voltage/current is in the opposite polarity since the flow of this charge carrier is in opposite direction. However, the voltage generated at this stage have lower and irregular values when comparing to the forward output signals.

In this study, five different devices were obtained (**Table 1.**): three of them had 7 conductive fibers each, one with 19 conductive fibers (as shown in **Figure 3.6c**) and another with 3 conductive fibers. Each device with 7 fibers had conductive fibers with different times of PPy polymerization. One device had the 30 minutes conductive fibers, the other had the 60 minutes and the last one had the 90 minutes. The conductive fibers present in the devices with 19 and 3 fibers had a PPy functionalization time of 30 minutes. Hence, we could compare how the results changed according to different PPy polymerization time of the fibers, and with a different number of fibers per device.

**Table 1**. *List of the harvesting devices produced during this work.*

| Device Name | Time of Polymerization | Number of Fibers |
|---|---|---|
| **7f_30 min** | 30 minutes | 7 |
| **7f_60 min** | 60 minutes | 7 |
| **7f_90 min** | 90 minutes | 7 |
| **3f_30 min** | 30 minutes | 3 |
| **19f_30 min** | 30 minutes | 19 |

Concerning the measurements of the $V_{oc}$, each device was directly connected to an oscilloscope, while the $I_{sc}$ measurement demanded each device to be first connected to a current-to-voltage converter. The evaluation of instant power and current output was done by connecting each device to various loads and examining the voltage while patting. This type of measurement was carried out during a time span of 5 months, to test the stability of the devices.

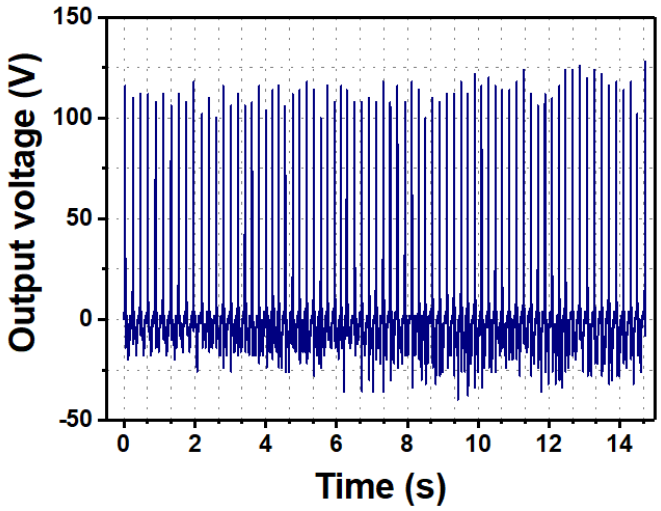


**Figure 3.7** *Open-circuit output voltage from the 7f_30min device.*

Regarding the 7-fibers devices, the average recorded output signals were slightly different depending on the PPy functionalization time. The 7f_30min device average open circuit voltage was 125.6 V, and the short circuit current was 8.5 µA, for the 7f_60min minutes device the average output signals were 129.3 V and

8.3 µA, and, for the 7f_90min device 124.9 V and 6.7 µA. From these results, we can see that the 7f_60min device had the higher average $V_{oc}$ and the 7f_30min device had the higher average $I_{sc}$, although the difference to the 7f_60min device is very small.

For the 19f_30min device, the average results of $V_{oc}$ and $I_{sc}$ were 244 V and 15 µA, respectively. For the 3f_30min device, the $V_{oc}$ is 49.8 V and the $I_{sc}$ is 3.2 µA (**Figure 3.8**). Comparing these results with the 7f_30min device, for the 19f_30min device the $V_{oc}$ almost doubled and the $I_{sc}$ also increased consistently. Comparing the 3f_30min device with the 7f_30min device results, the $V_{oc}$ decreased more than half and the $I_{sc}$ was aproximately one third. All these results were quite expected, demonstrating that with the increase of the number of fibers in one device, the corresponding $V_{oc}$ and $I_{sc}$ increase as well. In this study, we could not conclude if there exists a specific function between the number of fibers per device and corresponding $V_{oc}$ and $I_{sc}$. To reach that conclusion, we would have needed a vast amount of data, which we do not have due to time concerns. To find the behavior function between the number of fibers and the outputs $V_{oc}$ and $I_{sc,}$ more devices with different number of fibers should be constructed.

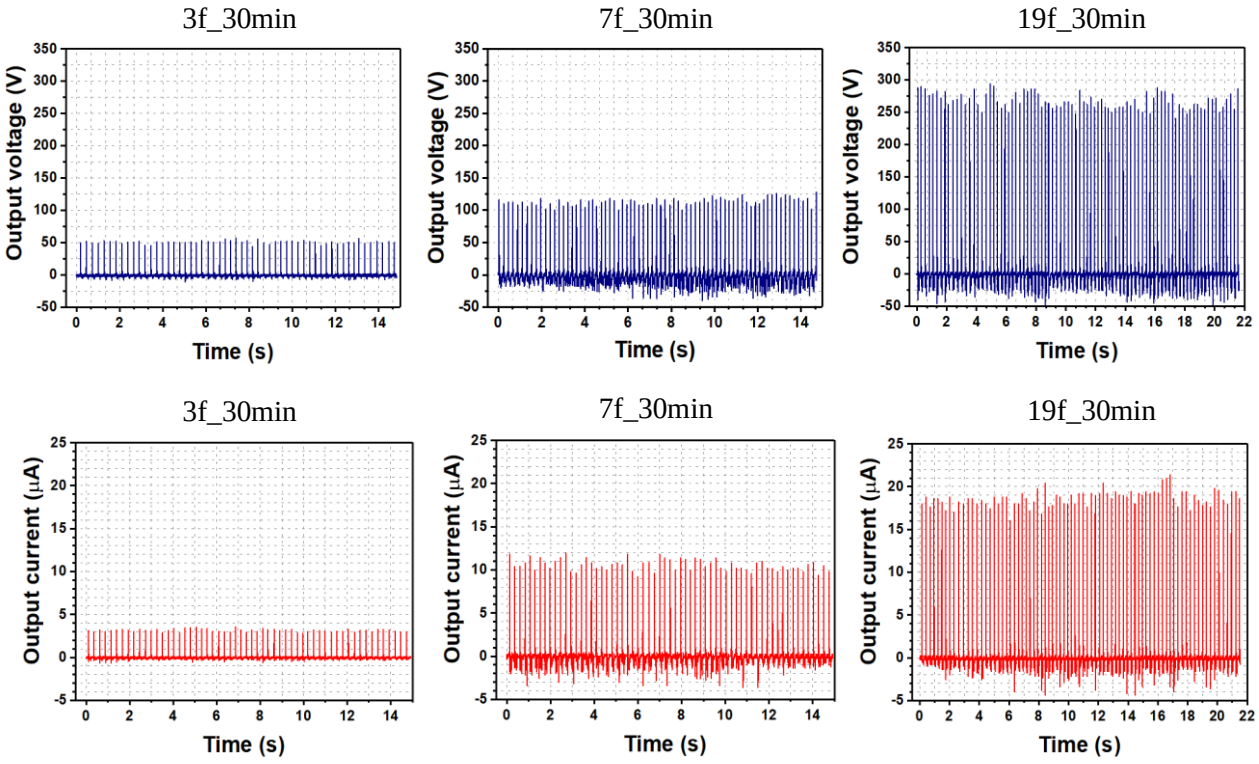


**Figure 3.8** *Average output voltage and current graphs of the devices namely, 3f_30min, 7f_30min, and 19f_30min, respectively from left to right.*

The real applications of any electrical device are associated with its power density and efficiency. A rectifier was added to the circuit to obtain a DC output signal, since the energy harvested directly from the device is an AC signal. To calculate the power density of the devices, we added different external resistances to the rectifier circuit and recorded the instantaneous output voltage of the system. The load added ranged from 55kΩ to 150MΩ (twenty-eight different loads). By having each voltage value associated with a different load, it is possible to calculate the power by the relation $P=V^2/R$, and then each result was divided by the area to get the power density. The area considered in these calculations was the external surface area of the fiber that is

coated with PPy. It is also important to note that the current density increases with the decrease of the external load in the circuit.

So, from the equation described above, the maximum results of power density and current density for the 7f_30min device are 0.85 W/m$^2$ and 22.4 mA/m$^2$, for the 7f_60min device are 0.52 W/m$^2$ and 14.2 mA/m$^2$, and for the 7f_90min device are 0.23 W/m$^2$ and 9.3 mA/m$^2$, respectively. Once more, we can observe that the 7f_30min device had a better performance in terms of power density and current density as well, while comparing with the other 7-fiber devices (**Figure 3.9**).

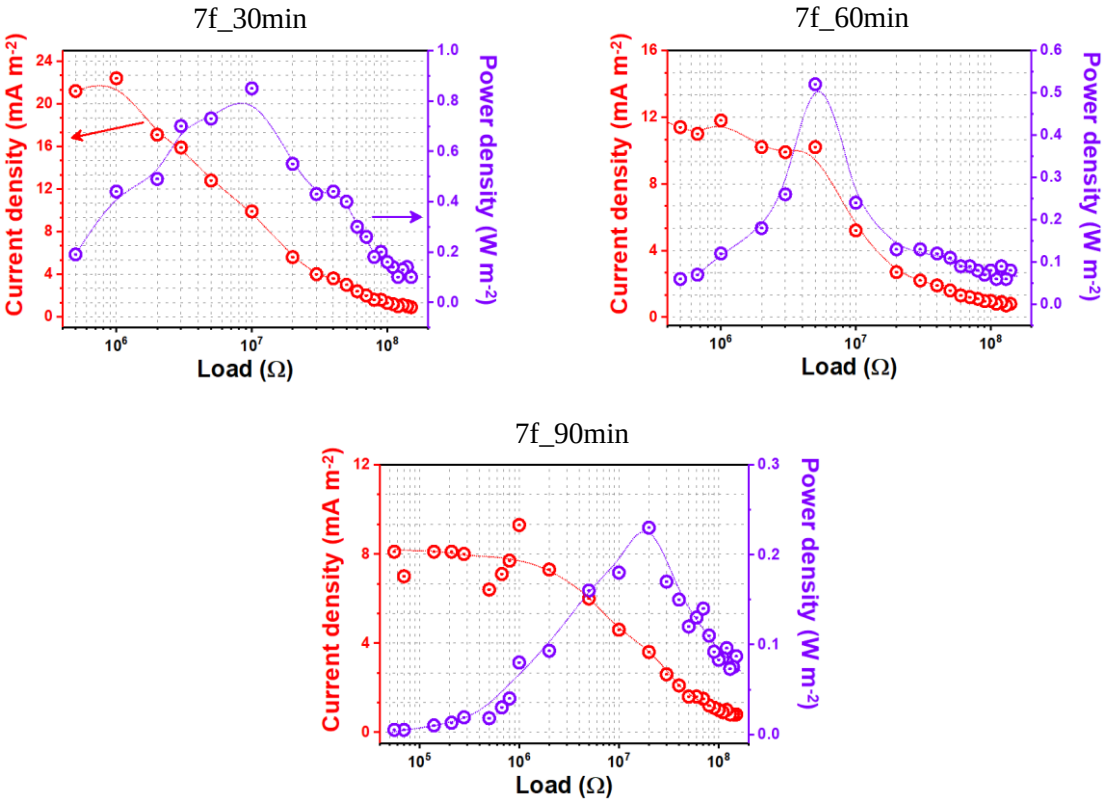


**Figure 3.9** *Power density and current density graphs of the 7f_30min, 7f_60min, and 7f_90min devices.*

Considering the 19f_30min device, the maximum value recorded for power and current densities were 2.29 W/m$^2$ and 19.5 mA/m$^2$ respectively, whereas for the 3f_30min device, 0.23 W/m$^2$ and 23.9 mA/m$^2$ respectively (**Figure 3.10**). By including the 7f_30min device, we can conclude that the maximum power density increases with the number of fibers and the maximum current density is approximately the same for all these three devices.

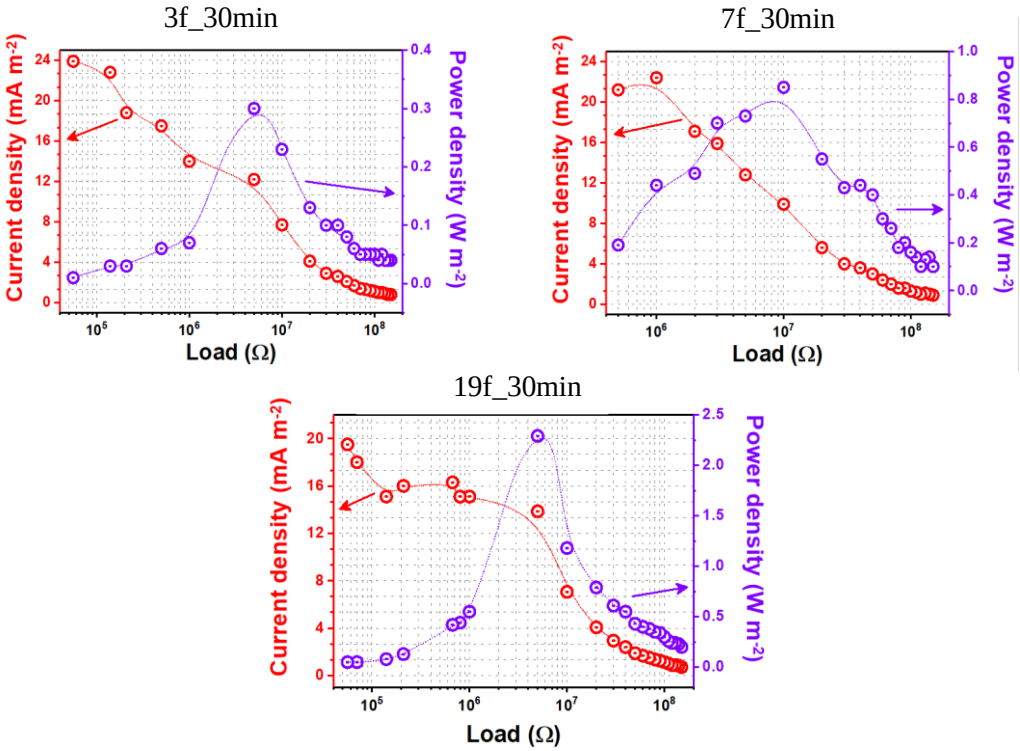


**Figure 3.10** *Power density and current density graphs of the 3f_30min, 7f_30min, and 19f_30min devices.*

Using the rectifier circuit to have a DC output we charged a commercial 33 µF capacitor. With simple hand patting on the 7-fibers devices, the power delivered from our 7f_30min device can charge the 33 µF commercial capacitors to 1 V in 306 s (5 minutes and 6 seconds), while the 7f_60min device took 449 s (7 minutes and 29 seconds) and the 7f_90min device took 930 s (15 minutes and 30 seconds). The 19f_30min device managed to do the same in just 225 s (3minutes and 45 seconds). Again, as expected, the time to charge the capacitor was way less for the 19f_30min device while compared to the 7-fibers devices.

Thirty (30) commercial blue LEDs (20 mA rating, 5mm diameter and 8.6mm height) were also powered by instantaneous hand patting, using the 7f_30min device (**Figure 3.11**), without the need of a commercial capacitor. Moreover, ten (10) blue LEDs were also powered by the 7f_60min and 7f_90min devices, separately. Using the 19f_30min device, fifty (50) LEDs were powered by instantaneous patting as well. All the LEDs were connected in series during these experiments.

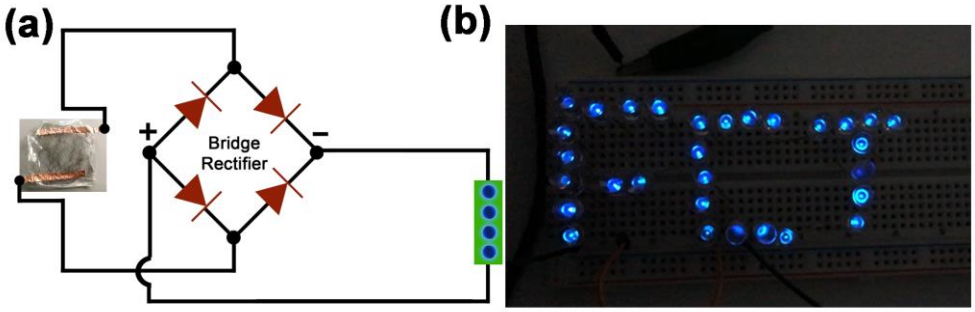


**Figure 3.11** *Snapshot of LEDs lighting up during performance tests of the 7f_30min device.*

## 3.3 Stability Test

Throughout the study period, the different 7-fiber devices were continuously tested in terms of $V_{oc}$ and $I_{sc}$, to check their stability in the ambient environment. All the devices were tested the same way (with the same testing setup and the same time intervals in-between tests for each device). The first measurement was right after the creation of the device, the second was one week after, the third three months later, the fourth four months later, and the fifth five months later. **Table 2** and **Table 3,** presented below, show the average results corresponding to each measurement done for $V_{oc}$ and $I_{sc}$ of the 7f_30min, 7f_60min, and 7f_90min devices. The discrepancy between the second and third tests was due to the Covid-19 lockdown. Ideally, after the first week, tests were planned to be performed every month up until the last month.

The numbers of $V_{oc}$ fluctuated ± 30 V for the 7f_30min device, ±50 V for the 7f_60min device, and ± 40 V for the 7f_90min device. Considering $I_{sc}$, the values fluctuate ± 4 µA for the 7f_30min device, ± 6 µA for the 7f_60min device, and ± 3 µA for the 7f_90min device. Since this fluctuation did not have a decreasing tendency with time, it could be caused by external factors such as humidity in the air or room temperature at the time of measurements. These factors can change/affect the resistance of the PPy [44] that eventually can change the performance of the devices.

In terms of $V_{oc}$, the 7f_30min device has the lowest fluctuation of them all, but in terms of $I_{sc}$, the device with less fluctuation was the 7f_90min device. With this scenario, we looked at the overall performance of the 7f_30min and the 7f_90min devices and found that the 7f_30min device had a higher average $V_{oc}$ and $I_{sc}$ than the 7f_90min device. After the first measurement, the 7f_30min device had always a higher $V_{oc}$ and $I_{sc}$ than the 7f_90min device, and in the last three measurements (from the third month to the fifth month) it had the best results of the three devices. Furthermore, the 7f_30min device was much more cost-effective than the other devices because it took less time to functionalize the fibers.

Having in mind all the factors described above, it is possible to conclude that all the devices are quite stable during the time of the study and every device was working properly until the end of the tests. However, it is also possible to observe that the 7f_30min device was the best in this test since it not only remained stable but improved its performance overtime, having the higher values of the $V_{oc}$ and $I_{sc}$ from all the devices, during the last three measurements.

**Table 2.** *Average results obtained in open circuit voltage ($V_{oc}$) tests performed for the 7-fiber devices throughout the work period.*

| Devices | 1st test | 1 week | 3 months | 4 months | 5 months |
|---|---|---|---|---|---|
| **7f_30min** | 113 V | 113 V | 140 V | 126 V | 137 V |
| **7f_60min** | 160 V | 122 V | 134 V | 107 V | 123 V |
| **7f_90min** | 147 V | 109 V | 134 V | 112 V | 123 V |

**Table 3.** *Average results obtained in short circuit current ($I_{sc}$) tests performed for the 7-fiber devices throughout the work period.*

| Devices | 1st test | 1 week | 3 months | 4 months | 5 months |
|---|---|---|---|---|---|
| **7f_30min** | 5.6 µA | 8.8 µA | 9.5 µA | 9.3 µA | 9.3 µA |
| **7f_60min** | 11.5 µA | 7.5 µA | 8.5 µA | 5.4 µA | 8.6 µA |
| **7f_90min** | 5.7 µA | 5.9 µA | 8.1 µA | 5.5 µA | 8.4 µA |

## 3.4 Bending Test

To test the sensing ability of the textile fibers functionalized with PPy, a very simple bending test was performed. Herein, a PDMS encapsulation was made to support just one functionalized fiber. The fiber with the PDMS encapsulation was attached to the finger (using lab gloves) and then was connected to an oscilloscope to check the instantaneous output voltage variation with opening and closing of the hand. **Figure 3.12** shows the peaks formed upon the bending of the fiber, when the hand was closed.

The test consisted in bending the fiber into different angles to see how the sensing ability was affected by different types of bending. The angles of bending used in this test were 45°, 90° and 180° (closed hand). The average $V_{oc}$ result of the 45° bending is around 495 mV, with a maximum recorded of 1 V. The average $V_{oc}$ result of the 90° bending was around 570 mV, with a maximum recorded of 1 V. For the 180° bending, the average $V_{oc}$ result was 830 mV and the maximum peak recorded went up to 2 V. These are very promising results, considering that this test was carried out with just one fiber and not a system of multiple fibers. Most importantly, this feature can be further developed for gesture monitoring.

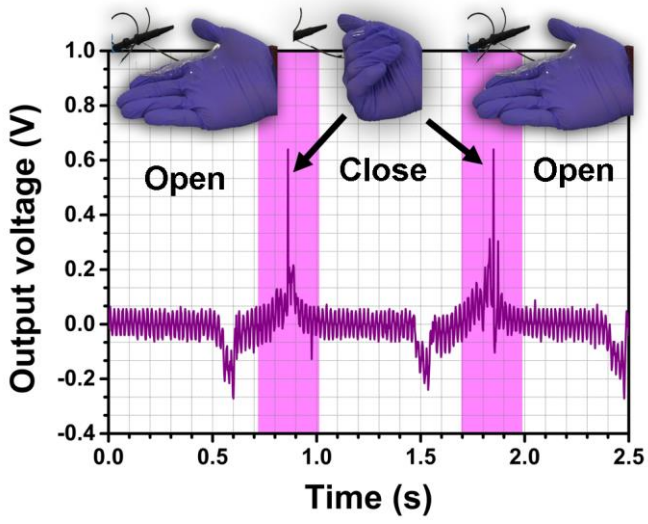


**Figure 3.12** *Output voltage graph from the 90° bending test where the peaks represent the maximum voltage obtained with the bended PPy functionalized fiber (fixed with finger).*

## 3.5 Real-Field Applications

### 3.5.1 Fabrication of the Weaved fabrics

Two different devices were made using the 1-meter PPy functionalized fibers.

The first device, namely D-MM (Device Metal Metal), was composed of one thicker (400 µm diameter) 1-meter PPy functionalized silver coated fiber that acted like the base of the fabric and one thinner conductive silver fiber (125 µm diameter) not functionalized (**Figure 3.13 b**). The goal was to weave the thinner fiber between the 1-meter fiber. Thus, a custom-made weaving machine, especially projected for this study, was developed in a 3D-printer (Ultimaker$^{2+}$). In this system, the 1-meter fiber was stuck to the edges, in a snake-like format. Then, with a needle, the thinner fiber is weaved in a perpendicular direction to the 1-meter fiber, also in a snake-like format (**Figure 3.13 a**). The thinner fiber is then used as the stress-deliver-charge-collector electrode and the 1-meter functionalized fiber as the back electrode.

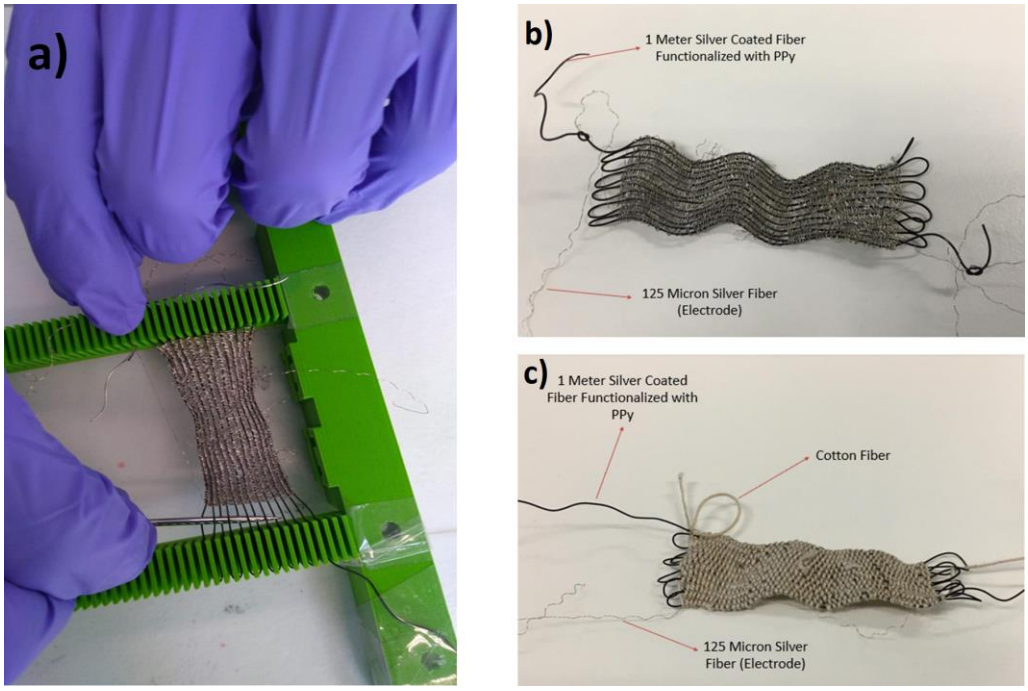


**Figure 3.13** *a) The custom-made weaving machine (green) and the process used to make the fabrics. Digital images of the created weaved devices: b) D-MM and c) D-MMC, respectively.*

The second device, namely D-MMC (Device Metal Metal Cotton), is composed of one 1-meter PPy functionalized fiber (400 µm diameter), that was the base of the fabric, and two other fibers that were weaved alternately in the 1-meter fiber: one thinner silver fiber (125 µm diameter) not functionalized, and one cotton fiber not functionalized (**Figure 3.13 c**). The thinner silver fiber acted like the electrode, while the cotton fiber was implemented (perpendicular to the 1-meter fiber and interspersed with the thinner fiber) to simulate a real fabric and to test the performance of the device in this condition.

### 3.5.2 Electrical Analysis of Weaved Fabrics

For the weaved devices, we made the same measurements that were made for the harvesting fiber devices: $V_{oc}$, $I_{sc}$, power and current density, and the capacitor charging test (**Figure 3.13**).

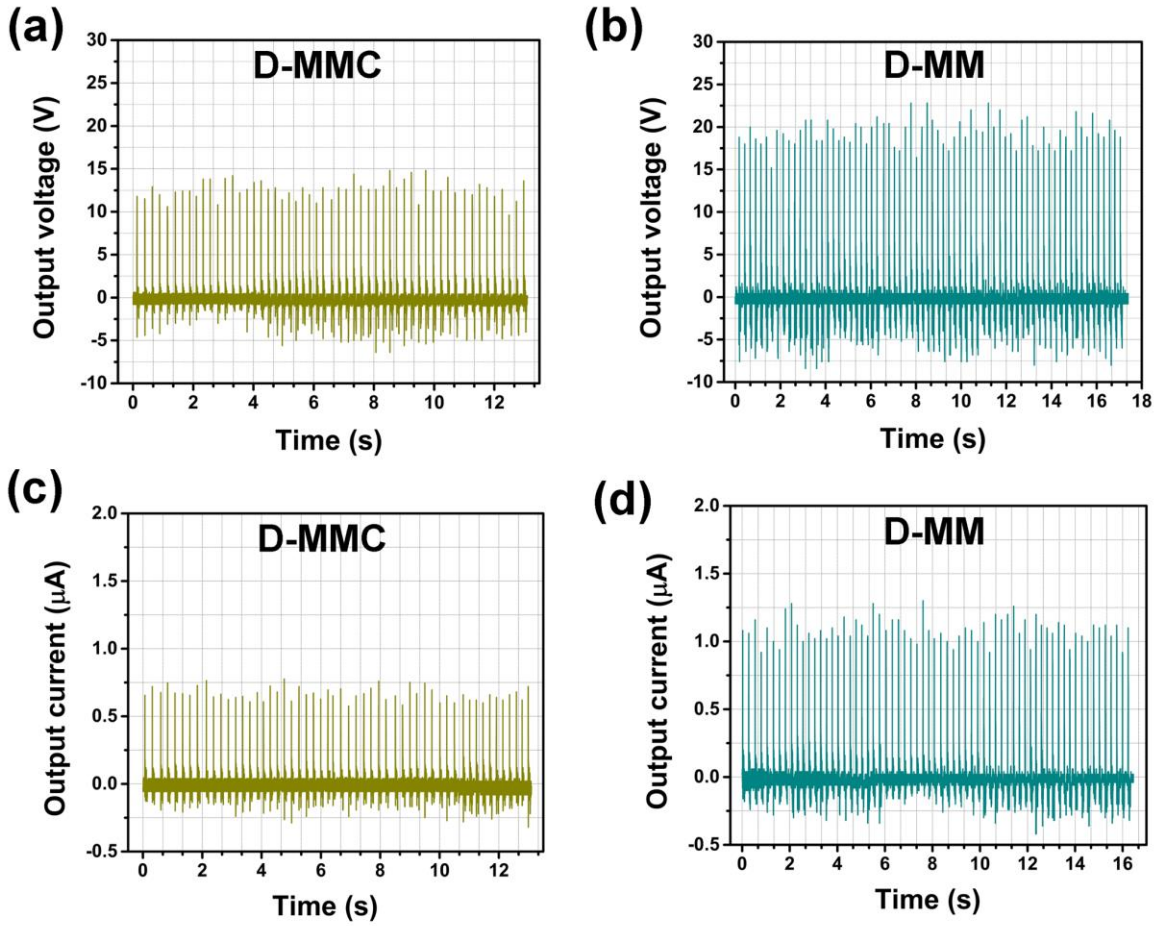


**Figure 3.14** *Average output voltage and current graphs of the weaved devices.*

In terms of $V_{oc}$ and $I_{sc}$ analyses, the average results of the D-MM device were 19.5 V and 1.02 µA, and the results of the D-MMC were 12.9 V and 0.62 µA, respectively.

The maximum results obtained for power density were 0.028 W/m$^2$ for the D-MM device and 0.04 W/m$^2$ for the D-MMC device. In terms of the current density, the maximum results were 9.17 mA/m$^2$ for D-MM and 11.6 mA/m$^2$ for D-MMC.

To charge 0.1 V on a 10 µF capacitor the D-MM device took 7min 30 seconds, whereas for D-MMC it took 5 min 22 seconds.

Hence, the functionalized weaved fabrics did not lose any significant electrical properties while incorporated into a cotton structure, which is quite positive in this case, proving that our system has the potential to be integrated in an e-textile application.

### 3.5.3 Wireless System Applications

One of the main focuses of this master thesis was to exhibit the ability and/or prospects of fiber-based devices for several types of real-world applications. A particular electronics strategy was employed in the applications that will follow. First, I would like to go into the strategy employed.

The overall strategy employed in all these applications was the use of a platform (either ESP32® or Arduino Uno®) to read the analog signals from the fibers prototypes and translate them to digital signals. It was always our goal to employ these applications into the IoT paradigm. For that, we used the ESP32, which is a platform like Arduino Uno that has larger specifications (for example, more analog pins, more internal memory, etc.) and an incorporated Wi-Fi and Bluetooth module. Therefore, we used the ESP32 hardware to setup an HTTP communication system, to exchange data without connecting it to a World Wide Web protocol. The ESP32 creates its own Asynchronous Web Server, where other devices can access by using the correct password. We can program the board with the exact Wi-Fi server name and password we want (For example, SSID: "Polypyrrole Device Test" and Password: "CENIMAT/I3N"). Arduino IDE® software was used to write the code to program both the Arduino Uno and ESP32. During this process, some ESP32 modules did not upload the sketches automatically, giving out the following error: "*Failed to connect to ESP32: Timed out waiting for packet header*". A 10 μF capacitor, with the positive side attached to the Enable pin and the negative side attached to the board's ground, was used to correct this error. The ESP32 can only use 4 pins for analog to digital conversion while having the Wi-Fi network online. Therefore, for applications with 5 or more inputs, we have used an Arduino Uno to read and convert the analog signals, establishing a UART (Universal Asynchronous Receiver-Transmitter) connection with the ESP32. In other words, the ESP32 and Arduino were transmitting data to one another directly (through a wire). That way, the ESP32 could send multiple sensor readings to the Asynchronous Web Server without the need to read them directly. For that, it was important to have the Transmitting Line of the Arduino connected to a Receiving Line of the ESP32 and vice-versa. While going for a UART connection it was important to bear in mind that the Arduino Uno's working voltage was different from the ESP32's. So, the signal that came from the transmitting line of the Arduino Uno (5V), had to be converted, in this case using a voltage divider, to the working voltage of the ESP32's (3.3V). Only then a stable UART connection was established successfully.

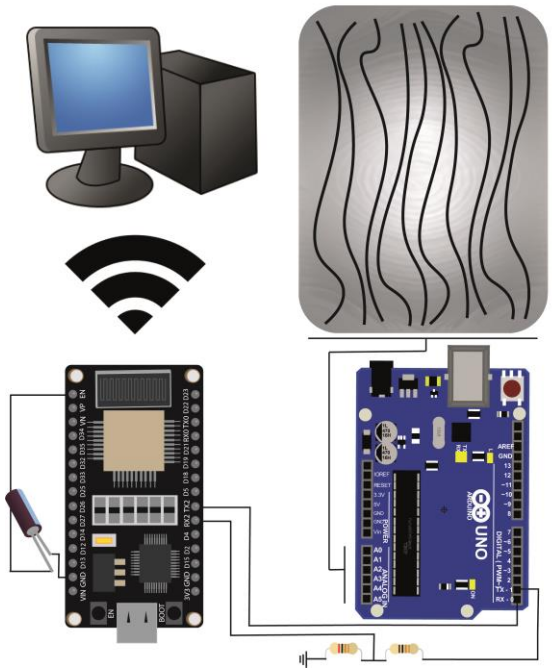

**Figure 3.15** *Schematic of the overall strategy employed for all the applications including an analog part (Polypyrrole devices), an analog-digital converter (Arduino or ESP32), Wi-Fi module (ESP32) and the final reading platform (PC).*

1. Sensing Security System with Human Interface – In this case, we used specific body parts (knee, elbow, and neck), and the devices produced during this thesis. We had one device attached to each body part and each device was also attached to its own Arduino board pin. By moving one body part (for example, bending the knee) the sensor reading will be associated with a particular pin. Readings from each pin will be either binary 1 (if the voltage reading > 100, which results from movement detection) or binary 0 (if voltage reading < 100, which results from no movement detection). The comparative value in the programming code

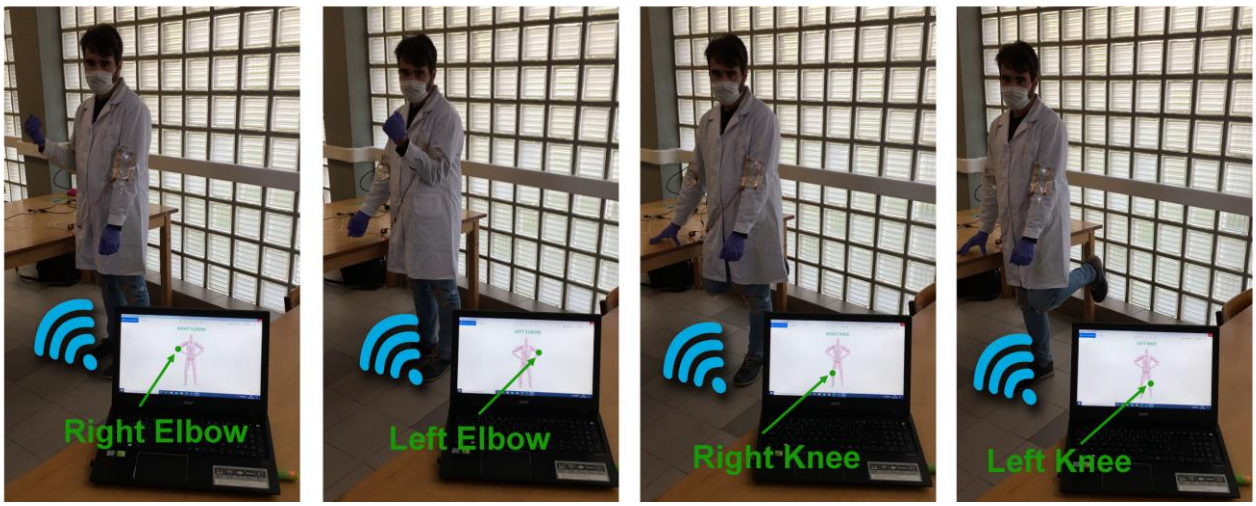


**Figure 3.16** *Still image of the investigation of gesture monitoring control through wireless technology and textile-based energy harvesting system.*

was 100 and not 0 to account for noise values. At this point, one binary value was associated with a variable that was associated with each pin GPIO. The ESP32 would then send these values to the webserver which was accessed by connecting to a particular link. Using Python software, we could access the mentioned link, get the binary values, and translate them to the desired output. This system could be used as a security system. For example, if you move four body parts in a particular order, it will unlock the system we want to have access to.

2. Force Sensor – To fabricate a force sensor prototype, we programmed the ESP32 to read the voltage from the fiber-based devices that were produced in this work. As we know from previous studies, the electrical performance of the devices also depends on the mechanical pressure applied. More mechanical pressure (in magnitude) will result in higher voltage and current signals. The ESP32 will then send the voltage reading to an online network, which is then read and interpreted by Python software to give out a particular output, depending on the magnitude of the voltage received (and consequently, depending on the magnitude of the force employed).

3. Movement Tracking System – This system captures the movements of a small Hot Wheels® car. Some fibers were evenly spaced out on top of a table. When the car passed on top of the fiber, it sent out a signal to the ESP32, which then send out the reading through a Web Server to another user. By using the Python software, the readings of ESP32, sent to the online server, are translated to either: distance covered or average speed. This application was still in development by the time this thesis was written (**Annex 3.**).

# 4 Conclusions and Future Perspectives

In this study, a new concept of mechanical energy harvesting and sensing system was made, with the purpose of being flexible, cheap, and convenient in day-to-day use, while generating renewable energy. Commercial silver coated textile fibers were used as the base for the devices. The textile fibers were coated with a conjugated polymer, so-called Polypyrrole, that provided the charge carriers generation with movements, needed for the the mechanical harvesting system formation.

Five harvesting devices were produced during this work, varying different factors. One of the factors was the functionalization time of the fibers with PPy. Three different times were tested in 7-fibers devices: 30 minutes, 60 minutes, and 90 minutes. One conclusion that can be brought out after carefully analyzing the results is that the 30 minutes PPy functionalized fibers were more stable (in terms of electrical performance) and have better power and current densities (0.85 $W/m^2$ and 22.4 $mA/m^2$) than the 60 or 90 minutes PPy functionalized fibers. The stability was measured over the $V_{oc}$ and $I_{sc}$ values of the devices throughout the time of the study (five different measurements).

Another factor that was studied during this thesis was the change in the electrical performance of devices with different number of fibers. Again, three different devices were made: one was composed of 3 fibers, the other with 7 fibers, and the last one with 19 fibers (all with 30 minutes PPy functionalized fibers). As expected, the electrical performance of the 19-fiber device was the best in terms of $V_{oc}$, $I_{sc}$ and power density, while the 3-fiber device was the worst in these parameters. With these results in mind, we can conclude that the $V_{oc}$, $I_{sc}$ and power density increased with the increase of the number of fibers in one device. The maximum power density achieved in this study was 2.29 $W/m^2$ (19-fiber device) and the maximum current density was 23.9 $mA/m^2$ (3-fiber device). The higher average $V_{oc}$ and $I_{sc}$ were 244 V and 15 µA, respectively (19-fiber device). The 19-fiber device was able to light up 50 commercial blue LEDs and charge a 33 µF commercial capacitor to 1 V in 225 s, by constant hand patting.

To test the implementation of these type of devices in real fabric applications, two more devices were made: D-MM (device not incorporated within cotton) and D-MMC (device incorporated within cotton). Here, the best results recorded in terms of power and current densities were from the D-MMC device with 0.04 $W/m^2$ and 11.6 $mA/m^2$, respectively, but the higher $V_{oc}$ and $I_{sc}$ average corresponded to the D-MM device (19.5 V and 1.02 µA). The results indicate that the devices are stable enough for e-textile applications.

It is important to note that prototyped wireless systems for force sensing, sensing with human interface, and movement tracking, were made using the fiber-based devices, an Arduino board, an ESP32 microcontroller and Python programming.

Even though the results of this study were positive and satisfying, there are always room for improvement and new investigations that can be done for further and continuous development of this work.

The merging of the fiber-based mechanical energy harvesting devices with fiber-based storage devices (such as supercapacitors) in an all-in-one device can have a lot of new and improved applications. This type of device is most likely to be used than the energy harvester device alone. This combination can bring a wide range of real-life applications that have a lot of demand in the current days.

Nanostructures where polypyrrole chains are organized are expected to have improved conductivity. So, trying to achieve other types of polypyrrole nanostructures, like nanotubes or nanowires and check how that affects the performance of the devices in opposition to the granular structure is another possible interesting study.

Fiber-based power management strategies should be developed to promote the energy conversion efficiency of the devices and provide a stable DC power supply for fiber-based self-powered systems.

In our case, the devices were based on the fiber substrate, and the stability and electrical performance depended a lot on the contact between the fiber and electrodes. In this study, we used copper tape to make the external electrodes of the devices, but sometimes this tape would not glue properly to the fibers, and the performance of the device was affected. If we find new ways to do better contact between the fibers and the external electrodes, we can bring a major improvement to the performances of such devices.

Hybridization of different mechanisms should be introduced in fiber-based devices to improve the device performance, like combining piezoelectric, electrostatic, and triboelectric effects together to harvest mechanical energy.

The study of the functionalization of other textiles is also important for future applications. Regarding this, a 1-meter cotton fiber was functionalized with PPy in this work. Even though the results were not in the same range as the ones from the silver-coated textile fibers, this topic deserves further studies and improvement, since it brings a truly wearable alternative for real-life applications. Also, its easy scale-up process for mass production makes the functionalized cotton a very promising material for mechanical energy harvesting.

With the continuous study and breakthrough in mechanical energy harvesting, it is possible to implement these devices in everyday life and harvest energy just by walking, for example. For this, the application investigation of future works can be towards this goal, giving emphasis to human motion detection and human motion energy harvesting on a large scale, through the implementation of fiber-based energy harvesting devices in shoes, clothes, or even carpets and sofas and test their real-life application performances.

Also, in the applications section of this work, the Arduino and Python coding can be improved to achieve better output results and the electrical circuits themselves can be improved to enhance the wireless system capability.

# 5 Bibliography


[1] IEA (2019), Global Energy & CO2 Status Report 2019, IEA, Paris. https://www.iea.org/reports/global-energy-co2-status-report-2019
[2] The European Green Deal Investment Plan and Just Transition Mechanism explained, European Commission, Brussels, 14 January 2020. https://ec.europa.eu/commission/presscorner/detail/en/qanda_20_24 (accessed on 21st, April, 2020).
[3] Chapter 24 - Renewable Energy Sources, P.S.R. Murty, in Electrical Power Systems, 2017, Pages 783-800, Imprint: Butterworth-Heinemann, Published Date: 14th June 2017. https://doi.org/10.1016/B978-0-08-101124-9.00024-3
[4] KarimShaikh, F., Zeadally, S. (2016) Energy harvesting in wireless sensor networks: A comprehen-sive review. Renewable and Sustainable Energy Reviews 55, 1041-1054.
[5] Magno, M., & Boyle, D. (2017). Wearable Energy Harvesting: From body to battery. 2017 12th International Conference on Design & Technology of Integrated Systems In Nanoscale Era (DTIS). doi:10.1109/dtis.2017.7930169
[6] J.G. Betts, P. Desaix, E. Jhonson, O. Korol, D. Kruse, B. Poe, J.A. Wise, M. Womble, K.A. Young, Anatomy and Physiology, OpenStax, Houston, 2013.
[7] Stoppa, M., & Chiolerio, A. (2014). Wearable Electronics and Smart Textiles: A critical review. Sensors (Switzerland). https://doi.org/10.3390/s140711957
[8] Heo, J. S., Eom, J., Kim, Y. H., & Park, S. K. (2018). Recent Progress of Textile-Based Wearable Electronics: A Comprehensive Review of Materials, Devices, and Applications. Small. https://doi.org/10.1002/smll.201703034
[9] Global Smart Textile Market – Industry Analysis and Forecast (2019-2027) by Function, Process, End User, and Geography, https://www.maximizemarketresearch.com/market-report/global-smart-textile-market/28970/
[10] Somov, A., Alonso, E. T., Craciun, M. F., Neves, A. I. S., & Baldycheva, A. (2017). Smart textile: Exploration of wireless sensing capabilities. 2017 IEEE SENSORS. doi:10.1109/icsens.2017.8234058
[11] Covaci, C., & Gontean, A. (2020). Piezoelectric energy harvesting solutions: A review. Sensors (Switzerland). https://doi.org/10.3390/s20123512
[12] Fortunato, E., Correia, N., Barquinha, P., Costa, C., Pereira, L., Gonçalves, G., & Martins, R. (2009). Paper field effect transistor. Zinc Oxide Materials and Devices IV. https://doi.org/10.1117/12.816547
[13] J. Lowell & A.C. Rose-Innes (1980): Contact electrification, Advances in Physics
[14] Goswami, S., Santos, A., Nandy, S., Igreja, R., Barquinha, P., Martins, R., & Fortunato, E. (2019). Human-motion interactive energy harvester based on polyaniline functionalized textile fibers following metal/polymer mechano-responsive charge transfer mechanism. Nano Energy. https://doi.org/10.1016/j.nanoen.2019.04.012
[15] Wu, C., Wang, A. C., Ding, W., Guo, H., & Wang, Z. L. (2019). Triboelectric Nanogenerator: A Foundation of the Energy for the New Era. Advanced Energy Materials. https://doi.org/10.1002/aenm.201802906
[16] Hu, Y., & Zheng, Z. (2019). Progress in textile-based triboelectric nanogenerators for smart fabrics. Nano Energy. https://doi.org/10.1016/j.nanoen.2018.11.025
[17] Paosangthong, W., Torah, R., & Beeby, S. (2019). Recent progress on textile-based triboelectric nanogenerators. Nano Energy. https://doi.org/10.1016/j.nanoen.2018.10.036
[18] Le, T. H., Kim, Y., & Yoon, H. (2017). Electrical and electrochemical properties of conducting polymers. Polymers. https://doi.org/10.3390/polym9040150
[19] Ferreira, G., Goswami, S., Nandy, S., Pereira, L., Martins, R., & Fortunato, E. (2020). Touch-Interactive Flexible Sustainable Energy Harvester and Self-Powered Smart Card. Advanced Functional Materials. https://doi.org/10.1002/adfm.201908994
[20] J. Y. Lee, S. H. Cho, and K. T. Song, Handbook of Conductive Polymers, T. A. Skotheim and J. R. Reynolds, Eds., CRC Press, New York, USA, 2007.
[21] P. Chandrasekhar, Conducting Polymers, Fundamentals and Applications: A Practical Approach, Springer Publications, New York, USA, 1999.
[22] Yussuf, A., Al-Saleh, M., Al-Enezi, S., & Abraham, G. (2018). Synthesis and Characterization of Conductive Polypyrrole: The Influence of the Oxidants and Monomer on the Electrical, Thermal, and Morphological Properties. International Journal of Polymer Science. https://doi.org/10.1155/2018/4191747
[23] Shi, Y., Peng, L., Ding, Y., Zhao, Y., & Yu, G. (2015). Nanostructured conductive polymers for advanced energy storage. Chemical Society Reviews. https://doi.org/10.1039/c5cs00362h
[24] Boroumand, F. A., Fry, P. W., & Lidzey, D. G. (2005). Nanoscale conjugated-polymer light-emitting diodes. Nano Letters. https://doi.org/10.1021/nl048382k
[25] Kim, B. H., Park, D. H., Joo, J., Yu, S. G., & Lee, S. H. (2005). Synthesis, characteristics, and field emission of doped and de-doped polypyrrole, polyaniline, poly(3,4-ethylenedioxythiophene) nanotubes and nanowires. Synthetic Metals. https://doi.org/10.1016/j.synthmet.2005.02.012

[26] Wang, C., Wang, Z., Li, M., & Li, H. (2001). Well-aligned polyaniline nano-fibril array membrane and its field emission property. Chemical Physics Letters.https://doi.org/10.1016/S0009-2614(01)00509-7
[27] Yan, H., Zhang, L., Shen, J., Chen, Z., Shi, G., & Zhang, B. (2006). Synthesis, property and field-emission behaviour of amorphous polypyrrole nanowires. Nanotechnology. https://doi.org/10.1088/0957-4484/17/14/017
[28] Cho, S. Il, Kwon, W. J., Choi, S. J., Kim, P., Park, S. A., Kim, J., … Lee, S. B. (2005). Nanotube-based ultrafast electrochromic display. Advanced Materials. https://doi.org/10.1002/adma.200400499
[29] Cho, S. Il, Xiao, R., & Lee, S. B. (2007). Electrochemical synthesis of poly(3,4-ethylenedioxythiophene) nanotubes towards fast window-type electrochromic devices. Nanotechnology. https://doi.org/10.1088/0957-4484/18/40/405705
[30] Rajesh, Ahuja, T., & Kumar, D. (2009). Recent progress in the development of nano-structured conducting polymers/nanocomposites for sensor applications. Sensors and Actuators, B: Chemical. https://doi.org/10.1016/j.snb.2008.09.014
[31] Lange, U., Roznyatovskaya, N. V., & Mirsky, V. M. (2008). Conducting polymers in chemical sensors and arrays. Analytica Chimica Acta. https://doi.org/10.1016/j.aca.2008.02.068
[32] Ago, H., Petritsch, K., Shaffer, M. S. P., Windle, A. H., & Friend, R. H. (1999). Composites of carbon nanotubes and conjugated polymers for photovoltaic devices. Advanced Materials. https://doi.org/10.1002/(SICI)1521-4095(199910)11:15<1281::AID-ADMA1281>3.0.CO;2-6
[33] Michira, I., Akinyeye, R., Baker, P., & Iwuoha, E. (2011). Synthesis and characterization of sulfonated polyanilines and application in construction of a diazinon biosensor. International Journal of Polymeric Materials and Polymeric Biomaterials. https://doi.org/10.1080/00914037.2010.531815
[34] Geetha, S.; Rao, C.R.K.; Vijayan, M.; Trivedi, D.C. Biosensing anddrug delivery by polypyrrole. Anal. Chim. Acta2006,568,119–125.
[35] Nambiar, S., & Yeow, J. T. W. (2011). Conductive polymer-based sensors for biomedical applications. Biosensors and Bioelectronics. https://doi.org/10.1016/j.bios.2010.09.046
[36] Kim, S., Kim, J. H., Jeon, O., Kwon, I. C., & Park, K. (2009). Engineered polymers for advanced drug delivery. European Journal of Pharmaceutics and Biopharmaceutics. https://doi.org/10.1016/j.ejpb.2008.09.021
[37] Das, T. K., & Prusty, S. (2012). Review on Conducting Polymers and Their Applications. Polymer - Plastics Technology and Engineering. https://doi.org/10.1080/03602559.2012.710697
[38] Ilicheva, N. S., Kitaeva, N. K., Duflot, V. R., & Kabanova, V. I. (2012). Synthesis and Properties of Electroconductive Polymeric Composite Material Based on Polypyrrole. ISRN Polymer Science. https://doi.org/10.5402/2012/320316
[39] Kassim, A., Basar, Z. B., & Mahmud, H. N. M. E. (2002). Effects of preparation temperature on the conductivity of polypyrrole conducting polymer. Proceedings of the Indian Academy of Sciences: Chemical Sciences. https://doi.org/10.1007/BF02704308
[40] Vernitskaya, T. V., & Efimov, O. N. (1997). Polypyrrole: A conducting polymer (synthesis, properties, and applications). Uspekhi Khimii. https://doi.org/10.1070/rc1997v066n05abeh000261
[41] Liang, L., Chen, G., & Guo, C. Y. (2017). Polypyrrole nanostructures and their thermoelectric performance. Materials Chemistry Frontiers. https://doi.org/10.1039/c6qm00061d
[42] Ayad, M. M. (1994). Influence of HCL on polypyrrole films prepared chemically from ferric chloride. Journal of Polymer Science Part A: Polymer Chemistry. https://doi.org/10.1002/pola.1994.080320102
[43] Liu, Y. C., & Hwang, B. J. (2000). Identification of oxidized polypyrrole on Raman spectrum. Synthetic Metals. https://doi.org/10.1016/S0379-6779(00)00188-0
[44] Cho, J. H., Yu, J. B., Kim, J. S., Sohn, S. O., Lee, D. D., & Huh, J. S. (2005). Sensing behaviors of polypyrrole sensor under humidity condition. Sensors and Actuators, B: Chemical. https://doi.org/10.1016/j.snb.2004.12.082
[45] Tian, Z., He, J., Chen, X., Wen, T., Zhai, C., Zhang, Z., … Xue, C. (2018). Core-shell coaxially structured triboelectric nanogenerator for energy harvesting and motion sensing. RSC Advances. https://doi.org/10.1039/c7ra12739a
[46] Kim, K. N., Chun, J., Kim, J. W., Lee, K. Y., Park, J. U., Kim, S. W., … Baik, J. M. (2015). Highly Stretchable 2D Fabrics for Wearable Triboelectric Nanogenerator under Harsh Environments. ACS Nano. https://doi.org/10.1021/acsnano.5b02010
[47] Gu, L., Cui, N., Cheng, L., Xu, Q., Bai, S., Yuan, M., … Wang, Z. L. (2013). Flexible fiber nanogenerator with 209 v output voltage directly powers a light-emitting diode. Nano Letters. https://doi.org/10.1021/nl303539c
[48] Chen, X., Tian, H., Li, X., Shao, J., Ding, Y., An, N., & Zhou, Y. (2015). A high performance P(VDF-TrFE) nanogenerator with self-connected and vertically integrated fibers by patterned EHD pulling. Nanoscale. https://doi.org/10.1039/c5nr01746g
[49] Kim, S. J., We, J. H., & Cho, B. J. (2014). A wearable thermoelectric generator fabricated on a glass fabric. Energy and Environmental Science. https://doi.org/10.1039/c4ee00242c
[50] Cheng, Y., Lu, X., Hoe Chan, K., Wang, R., Cao, Z., Sun, J., & Wei Ho, G. (2017). A stretchable fiber nanogenerator for versatile mechanical energy harvesting and self-powered full-range personal healthcare monitoring. Nano Energy. https://doi.org/10.1016/j.nanoen.2017.10.010

# 6 Annexes

## Annex 1.

**Table 4.** *Recent literature survey of fiber-based energy harvesting devices and respective output results of the significant ones.*

| Fiber-based energy conversion device | Materials | Open Circuit Voltage (V) | Short Circuit Current (µA) | Power Density (mW $m^{-2}$) | Year of Publication |
|---|---|---|---|---|---|
| **FTENG** | Rubber-Ni | 380 | 11 | 869 | 2018 [45] |
| **FTENG** | PDMS-Au | 40 | 210 | 204 | 2015 [46] |
| **FPENG** | PZT | 209 | 53 | - | 2013 [47] |
| **FPENG** | P(VDF-TrFE) | 4 | 2.6 | - | 2015 [48] |
| **FTEG** | Bi2Te3–Sb2Te3 | 0.09 | - | 380 | 2014 [49] |
| **FENG** | PTFE-AgNWs | 0.66 | 0.02 | 0.0225 | 2017 [50] |
| **Charge Transfer Mechanism** | Polyaniline-Cu | 116 | 16 | 600 | 2019 [14] |
| **Charge Transfer Mechanism** | Polypyrrole-Cu (Present Work) | 244 | 15 | 2290 | 2020 |

The last two rows of **Table 4** show the results of our group, where textile fibers were functionalized with polyaniline (previous work), and polypyrrole (present work).

## Annex 2. Charge Transfer Energy Diagram

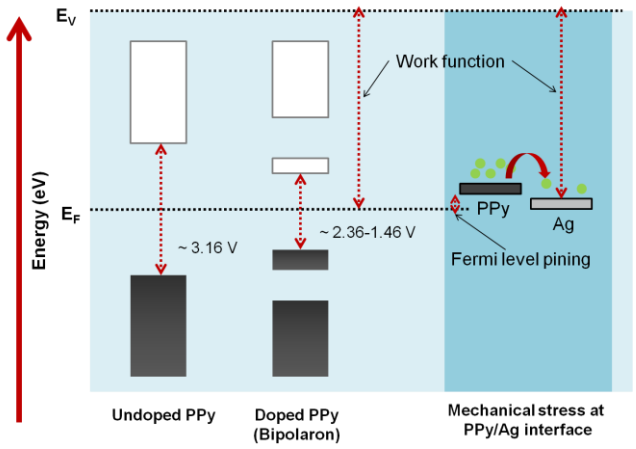


**Figure 6.1** *Charge Transfer Energy Diagram.*

# Annex 3. Movement Tracking System Application

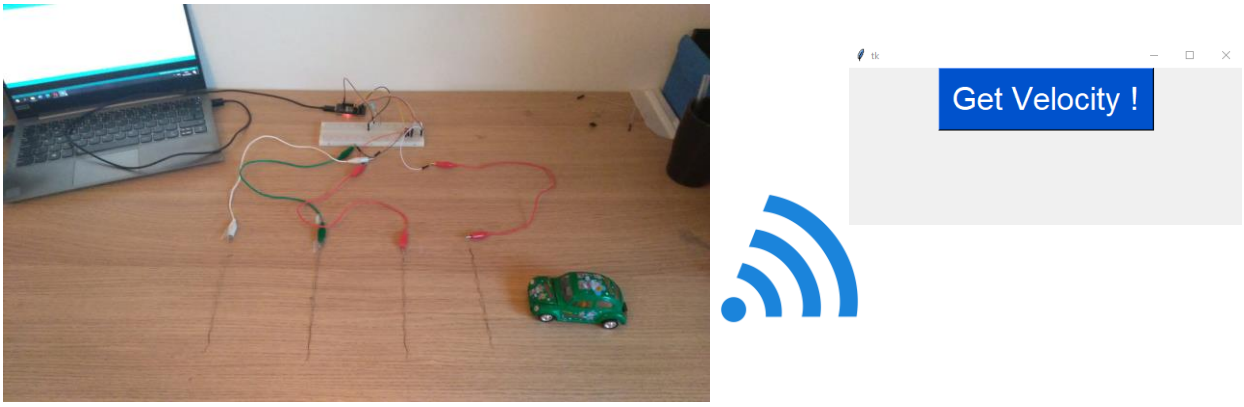


**Figure 6.2** *Movement Tracking System constructed and preview of the desired output.*

In **Figure 6.1** we can see the system that was already built and the intented output. The goal of this application is that when the toy car passes on top of the fibers it will send a signal to ESP32 to then be processed into distance traveled or average speed of the car. This data is sent to a Web Server. By running the output code (in another PC) we get the "window" showed in the **Figure 6.1**. By clicking in the button "Get Velocity!" the average velocity of the car is displayed. As said before, this application is still in development.

# Annex 4. Python Code

Python code of the Sensing Security System with Human Interface application is described below:

```
import requests
from PIL import Image
import matplotlib.pyplot as plt
import matplotlib.image as mpimg
import time
while True:

    # api-endpoint
    URL = "http://192.168.4.1/voltage1"
    # defining a params dict for the parameters to be sent to the API
    PARAMS = {'192.168.4.1':1}
    # sending get request and saving the response as response object
    r = requests.get(url = URL, params = PARAMS)
```

```
# extracting data in json format
data1= r.json()


# api-endpoint
URL = "http://192.168.4.1/voltage2"
# defining a params dict for the parameters to be sent to the API
PARAMS = {'192.168.4.1':1}
# sending get request and saving the response as response object
r = requests.get(url = URL, params = PARAMS)
# extracting data in json format
data2 = r.json()


# api-endpoint
URL = "http://192.168.4.1/voltage3"
# defining a params dict for the parameters to be sent to the API
PARAMS = {'192.168.4.1':1}
# sending get request and saving the response as response object
r = requests.get(url = URL, params = PARAMS)
# extracting data in json format
data3 = r.json()


# api-endpoint
URL = "http://192.168.4.1/voltage4"
# defining a params dict for the parameters to be sent to the API
PARAMS = {'192.168.4.1':1}
# sending get request and saving the response as response object
r = requests.get(url = URL, params = PARAMS)
# extracting data in json format
data4 = r.json()

word=[data1,data2,data3,data4]
print(word)
```

```
if word==[1,0,0,0]:
    im = Image.open(r"C:\Users\Coalhon88\Pictures\Saved Pictures\rightknee.png")
    im.show()
elif word==[0,1,0,0]:
    im = Image.open(r"C:\Users\Coalhon88\Pictures\Saved Pictures\leftknee.png")
    im.show()
elif word==[0,0,1,0]:
    im = Image.open(r"C:\Users\Coalhon88\Pictures\Saved Pictures\rightelbow.png")
    im.show()
elif word==[0,0,0,1]:
    im = Image.open(r"C:\Users\Coalhon88\Pictures\Saved Pictures\leftelbow.png")
    im.show()
else:
    print('WRONG INPUT')


time.sleep(5)
```

# Annex 4. Supporting Real-time Videos

1. Supporting Video SV1: Real-time video of instantaneous powering up 30 LEDs in series configuration by touch-interactive energy harvesting from self-powered device. https://drive.google.com/file/d/1KQ2cKtA35mhn0XhkORZmemX36dbgXsb-/view?usp=sharing
2. Supporting Video SV2: Sensing security system with human interface application real-time test. https://drive.google.com/file/d/1iICQdUna7GD8MUJE27QjmIhB1-kiXuML/view?usp=sharing